Palaeogeography, Palaeoclimatology, Palaeoecology 584 (2021) 110666

Contents lists available at ScienceDirect

Palaeogeography, Palaeoclimatology, Palaeoecology

journal homepage: www.elsevier.com/locate/palaeo

# Paleogeographic reconstruction of Mississippian to Middle Pennsylvanian basins in Nevada, southwestern Laurentia

Patricia H. Cashman [a], Daniel M. Sturmer [b,*]

[a] Department of Geological Sciences and Engineering, University of Nevada, Reno, 1664 N. Virginia St., Reno, NV 89557-0172, USA
[b] Department of Geology, University of Cincinnati, 500 Geology/Physics, Cincinnati, OH 45221-0013, USA

ARTICLE INFO

Editor: Thomas Algeo

*Keywords:*
Antler Orogeny
Laurentia
Palinspastic reconstruction
Nevada

ABSTRACT

Compilation of stratigraphic, sedimentological, and structural data on palinspastically restored maps reveals the Mississippian-Pennsylvanian paleogeography of Nevada in unprecedented detail, and has important implications for the development of the southwestern Laurentian margin. In contrast to previous interpretations of latest Devonian-earliest Mississippian tectonism, the maps show the major tectonic events to have been in late Middle Mississippian and Middle Pennsylvanian time. Regionally extensive unconformities mark both, with the deepest erosion in the northwest. Sub-unconformity structures record primarily NW-SE shortening, and synorogenic sediments were shed toward the east, southeast and south. These observations are consistent with protracted sinistral-oblique convergence in Nevada along the southwest Laurentian margin, rather than the W-E convergence invoked in previous interpretations. Terminology for late Paleozoic orogenies in Nevada must be revised accordingly.

## 1. Introduction

The western edge of southwestern Laurentia has previously been interpreted as a convergent plate boundary with shortening events in Late Devonian-Early Mississippian (Antler Orogeny) and Permian-Triassic (Sonoma Orogeny) time. Both orogenies are anomalous in their lack of associated igneous or metamorphic rocks. An early tectonic evaluation of the first, Late Devonian-Early Mississippian, event noted that although there was evidence for Paleozoic tectonic activity along the entire margin of North America, a major allochthon was present only in Nevada (Nilsen and Stewart, 1980). Subsequent studies of the sedimentary and structural evidence for Paleozoic tectonism in Nevada have revealed that structures, angular unconformities, and syntectonic strata do not reflect a simple allochthon-emplacement history (Fig. 1). We examine structural and paleogeographic data from the Mississippian to Middle Pennsylvanian basin deposits to re-evaluate the nature and evolution of the plate boundary in Nevada during this time. For simplicity, we refer to this as "late Paleozoic" throughout the paper, although the time interval described herein does not include Late Pennsylvanian or Permian time.

The Antler Orogeny (e.g., Roberts et al., 1958; Nilsen and Stewart, 1980) and Sonoma Orogeny (e.g., Silberling and Roberts, 1962; Roberts, 1968; Burchfiel and Davis, 1972; Snyder and Brueckner, 1983) were interpreted as eastward emplacement of oceanic rocks onto the Laurentian margin. The models were based on geologic relationships in Nevada. The "Antler Orogeny" as initially defined referred to Late Devonian – Early Mississippian (D/M) orogenic activity culminating with emplacement of the Antler Allochthon along the Roberts Mountains Thrust (RMT) (Roberts et al., 1958) (Fig. 2). However, the term has since been broadly applied to structures and synorogenic sedimentary rocks throughout the late Paleozoic, obscuring the distinction between, and significance of, the records from different time periods. Similarly, the term "Roberts Mountains Thrust" (Fig. 2) has typically been applied to any fault contact between oceanic rocks ("western assemblage" of Roberts et al., 1958) and continental margin rocks ("eastern assemblage" of Roberts et al., 1958), without considering evidence for its age, kinematics or regional significance. This, too, complicates recognition of the actual tectonic history. For example, there are no known cases where the "RMT" or structures associated with it are unequivocally D/M in age. In fact, the unconformably overlying "Overlap Assemblage" is as young as Pennsylvanian in many places, so the resulting hiatus is a highly imprecise age bracket (Fig. 3). In addition, post-Antler depositional basins and periods of tectonism in Nevada have been recognized to have existed at several times throughout the late Paleozoic (Fig. 1) (e.g., Dott

* Corresponding author.
*E-mail addresses:* pcashman@unr.edu (P.H. Cashman), Daniel.Sturmer@uc.edu (D.M. Sturmer).

https://doi.org/10.1016/j.palaeo.2021.110666
Received 31 May 2021; Received in revised form 31 August 2021; Accepted 16 September 2021
Available online 25 September 2021

Jr., 1955; Ketner, 1977; Trexler Jr. and Nitchman, 1990; Trexler Jr. et al., 2003, 2004; Cashman et al., 2011, and references therein). Other data indicate a significant sinistral component of offset across the late Paleozoic plate boundary (e.g., Stone and Stevens,1988; Walker, 1988; Linde et al., 2016, 2017; Lawton et al., 2017; Chen and Clemens-Knott, 2021; Key and Cashman, 2021).

In this study we reexamine the Mississippian – Middle Pennsylvanian rocks in Nevada that inspired the original, margin-perpendicular convergence interpretation, and compile structural and paleogeographic data that pertain to the nature and evolution of the late Paleozoic plate boundary. We have examined the Carboniferous sedimentary record in Nevada and compiled a series of palinspastically-restored maps from Kinderhookian to Desmoinesian (Early Mississippian to Middle Pennsylvanian) time. The paleogeographic maps depict depositional environment, paleocurrent, and compositional data for each time slice. The sub-unconformity maps display the extent and depth of erosion at unconformities, and, locally, the orientations of sub-unconformity structures formed during the associated crustal shortening. These maps are based on our unpublished sedimentological, paleocurrent and structural data as well as data from the literature. The base maps have been palinspastically restored to remove both Permian to early Cenozoic shortening (this paper), and Cenozoic extension and translation (McQuarrie and Wernicke (2005). The resulting maps represent a more accurate depiction of the depositional environments through time than was previously available.

In this paper, we present detailed paleogeographic time slices for Early Mississippian to Middle Pennsylvanian rocks in Nevada, then use them to clarify the tectonic development of the southwest Laurentian margin. We start with a brief summary of early tectonic models of the late Paleozoic in southwestern Laurentia, and the Antler Orogeny in particular, along with some of the anomalies and contradictions they entail. We then review further constraints from recent published data, from borehole geophysics to detrital zircon spectra, that refine our understanding of the upper Paleozoic rocks. We summarize the recognition criteria and ages of unconformities in the late Paleozoic record, illustrating our choice of time slices to map. We then present and explain our results, in new compilation maps for 8 time intervals: 1) Kinderhookian (early Antler Foreland Basin); 2) Osagean (Antler Foreland Basin); 3) C2 unconformity (sub-crop, Antler Successor Basin); 4) early Chesterian (early Antler Successor Basin); 5) late Chesterian (evolving Antler Successor Basin); 6) Atokan (Ely-Bird Spring Basin); 7) C5 unconformity (sub-crop, Hogan Basin); and 8) mid-Desmoinesian (Hogan Basin). We conclude with an updated interpretation of the evolution of southwestern Laurentia that includes a revised timing and significance of the "Antler Orogeny", recognition of the importance of post-Antler orogenic events, and reinterpretation of the southwestern Laurentian margin as a sinistral-oblique convergent boundary in late Paleozoic time.

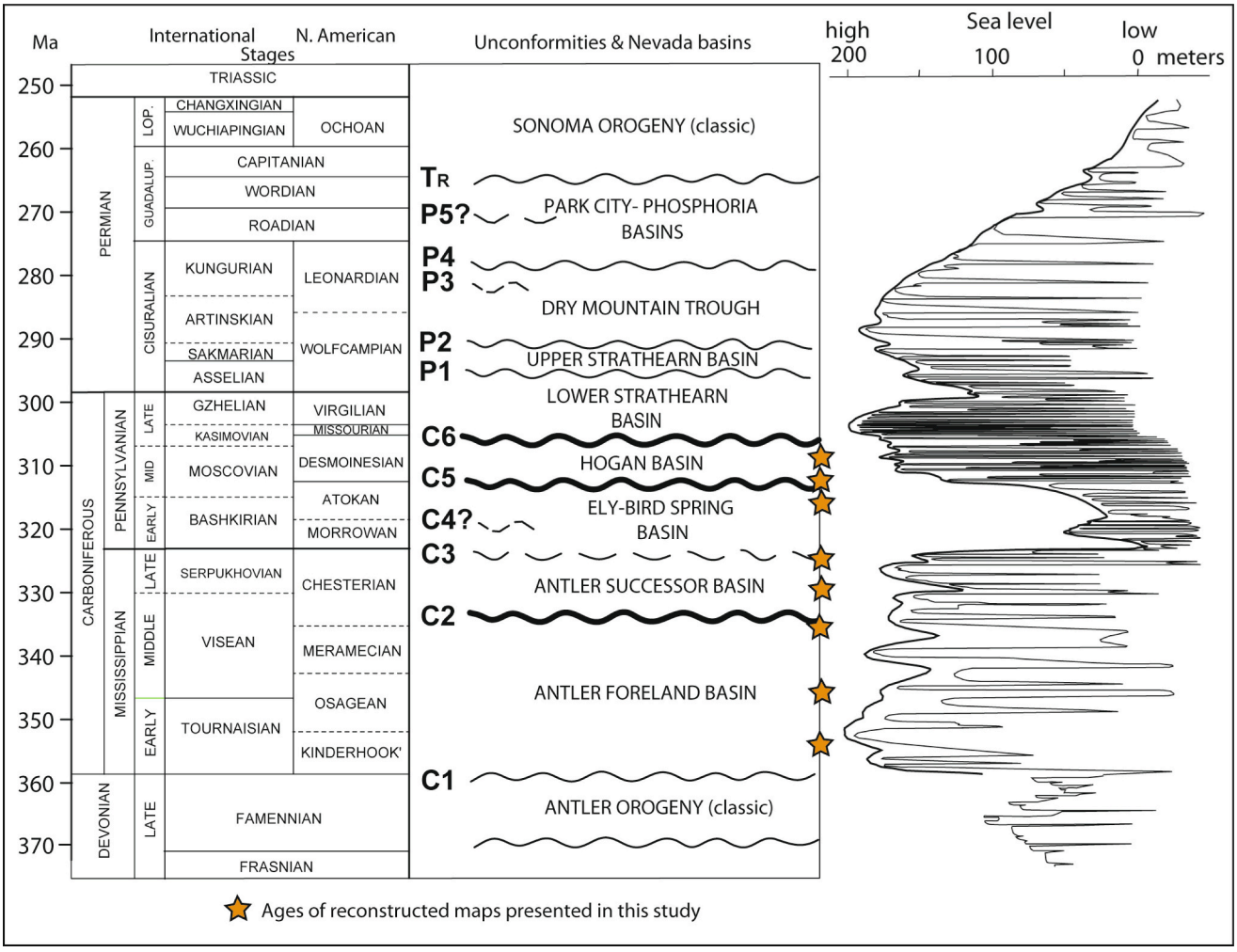


**Fig. 1.** Late Paleozoic basins, unconformities, and sea level curve. Unconformity diagram modified from Snyder et al. (2002) and Trexler Jr. et al. (2004). Sea level diagram shows high frequency sea level change (thin line) and a smoothed sea level curve (thick line). Sea level curve modified from Ross and Ross (1987) and Sandberg et al. (2002). Time scale from Henderson et al. (2020).

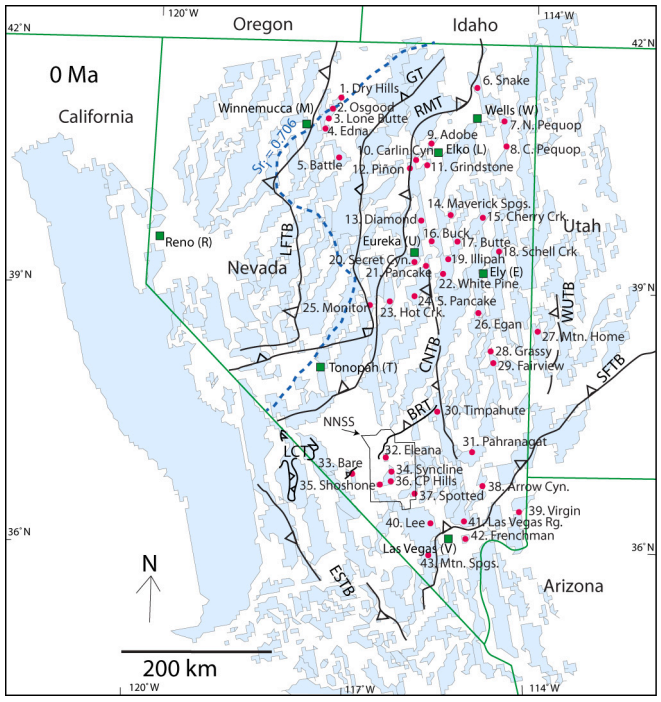


**Fig. 2.** Base map of present-day basins (white) and ranges (blue) with stratigraphic section control points (red dots). Cities (green squares) labeled on this map, are noted on other maps by the abbreviations shown in parentheses here. Thrust faults represent present position of frontal thrusts, from Snow and Wernicke (2000) and Long (2015). The "Roberts Mountains Thrust" trace was taken from published maps, and depicts the present eastern extent of oceanic rocks. It does not necessarily represent a single, continuous fault surface or imply a single age of emplacement. Initial Sr 0.706 line position from Grauch et al. (2003) BRT, Belted Range Thrust; CNTB; Central Nevada Thrust Belt; ESTB, Eastern Sierra Thrust Belt; GT, Golconda Thrust; LCT, Last Chance Thrust; LFTB, Luning-Fencemaker Thrust Belt; NNSS, Nevada National Security Site; RMT, Roberts Mountains Thrust; SFTB, Sevier Fold and Thrust Belt; . Map modified from McQuarrie and Wernicke (2005). (For interpretation of the references to colour in this figure legend, the reader is referred to the web version of this article.)

## 2. Background

The Antler Orogeny, defined in Nevada, formed a belt of "intense folding and thrusting that culminated in the Roberts Mountains Thrust fault (RMT) in Late Devonian or Early Mississippian time" (Fig. 2; Roberts et al., 1958). The RMT juxtaposed a western "eugeosynclinal" assemblage eastward or southeastward over the eastern "miogeosynclinal" rocks (Roberts et al., 1958). A 1979 Penrose Conference reaffirmed the timing and overall structure of the Antler Orogenic Belt in Nevada, while framing it in plate tectonic terms, i.e., an oceanic assemblage emplaced over a continental margin assemblage (Nilsen and Stewart, 1980). The term "Antler Orogeny" has subsequently been loosely invoked to explain a variety of late Paleozoic features in Nevada. To remove this source of confusion, in this paper, we *initially* restrict the term to the original usage sensu stricto, i.e., Late Devonian/Early Mississippian (D/M) tectonism. We will return to this topic at the end of this paper. Similarly, the term "Roberts Mountains Thrust" has been applied to the easily mappable fault boundary between oceanic and continental margin rocks, regardless of the age constraints on fault motion. For this case, however, we are forced to adopt the mapping-based definition because it is unambiguous, whereas the age of motion on a given segment of the mapped fault is not. We expressly note that this usage does *not* imply a unique, continuous fault surface or specific age of motion on the mapped fault. The RMT has not been described in Idaho, but syntectonic sedimentary deposits there have been attributed to the Antler Orogeny (e.g., Wilson et al., 1994; Link et al., 1996).

Anomalous and ambiguous aspects of the Antler orogeny have long been recognized. There is no D/M regional metamorphism in Nevada, and there are no associated D/M volcanic rocks. The relatively thin (2 km) stratigraphic section in the presumed foredeep near Eureka, Nevada (Trexler Jr. and Cashman, 1991) suggests that the tectonic load may have been either distant, or not large; however, strata far to the east were affected by subsidence (Trexler Jr. et al., 2003). Imprecise use of stratigraphic terms has complicated and obscured the record. For example, "Diamond Peak Formation" has been applied to conglomerates in turbidite deposits of the "Antler Foreland Basin", and to those in fluvial/deltaic deposits in the unconformably overlying "Antler Successor Basin". We use terms for basins sensu Ingersoll (2012): a "foreland basin" is a geographically relative term for a depositional basin in front of the related compressional mountain belt, without plate tectonic significance, and a "successor basin" is a basin that forms after the cessation of tectonic activity. In a region such as Nevada with repeated, overprinted tectonic events, modifiers are needed to distinguish between the basins; here, the modifier "Antler" refers to Mississippian rocks deposited immediately before and after Mississippian tectonism. Additionally, we retain these basin names as they are well-established in the literature. The "RMT" is not a single fault surface or fault zone. Where slip on the "RMT" surface can be dated, it is later than the D/M boundary (e.g., McFarlane, 1997; McFarlane, 2001; Key, 2015; Key and Cashman, 2021). Similarly, there are no structures of demonstrably D/M age in the RMT hanging wall or footwall. Structurally imbricated rocks are well documented both above and below the RMT (e.g., Saucier, 1995, 1997 and references therein; McFarlane, 1997), but field relations show that these structures post-date D/M time. Tight folds in the Ordovician Vinini Formation commonly attributed to the Antler Orogeny are constrained in age only by unconformably overlying "Antler Overlap Sequence" rocks. The "overlap" rocks are most commonly Pennsylvanian and Permian in age (e.g., Fig. 3, Saller and Dickinson, 1982), and thus do *not* restrict the folding to D/M time. Features attributed to the Antler Orogeny in south-central Idaho are also overlain by Middle Pennsylvanian rocks (Wilson et al., 1994).

In contrast, late Paleozoic structures and synorogenic clastic rocks that clearly *post-date* D/M time have been documented in Nevada for decades (Fig. 1). A prominent angular unconformity in Carlin Canyon separates the Chesterian Tonka Formation from the Missourian-Wolfcampian Strathearn Formation, recording "crustal instability" and considerable local erosion in Late Pennsylvanian time (Dott Jr., 1955). The Pennsylvanian rocks in Carlin Canyon are a western, more clastic, facies of the Ely Formation farther east in Nevada; Dott Jr. (1955) defined local stratigraphic names to acknowledge this difference and interpreted an orogenic source to the west. Silberling et al. (1997) documented Middle Mississippian deformation in central Nevada and related it to continuing Antler tectonism. A belt of Late Pennsylvanian - Permian orogenic sediments extending from southern California to Idaho was Ketner's (1977) evidence for a late Paleozoic "Humboldt Orogeny". He argued that the stark age difference between this and either the Antler or Sonoma Orogeny required the designation of a distinct orogeny. However, the broad age range of the rocks he cites undermines his interpretation that they represent a single event. Local fortuitous preservation of late Paleozoic rocks documents timing and kinematics for overprinted sets of late Paleozoic structures in several localities in northern Nevada (e.g., McFarlane, 1997, 2001; Sweet, 2003; Trexler Jr. et al., 2004; Villa, 2007; Siebenaler, 2011; Key, 2015; Key and Cashman, 2021; Whitmore et al., 2021).

Unconformities in the late Paleozoic section provide the key to unraveling the geologic history (Fig. 1). They represent genetically important breaks in the stratigraphic record (Snyder et al., 2000; Trexler Jr. et al., 2003). Biostratigraphic age control is essential; it brackets the age and lacuna of each unconformity and makes it possible to correlate unconformities from place to place. Importantly, the late Paleozoic unconformities can also be correlated laterally to "event horizons" (e.g.,

lithofacies shifts) that have the same origin (Trexler Jr. et al., 2003). This feature makes them useful far beyond the areas of actual uplift, deformation, and erosion (e.g., French et al., 2020). Similarly, the geometry and kinematics of structures underlying known unconformity surfaces (e.g., Trexler Jr. et al., 2004; Villa, 2007; Cashman et al., 2011) can suggest the age of similar structures elsewhere (e.g., Cole and Cashman, 1999; Sweet, 2003; Cashman et al., 2011; Russo, 2013; Key, 2015; Key and Cashman, 2021; Russo et al., 2021; Whitmore et al., 2021). Biostratigraphic control is generally at the sub-stage level (~1 Myr control) with foraminifera (including fusulinaceans), conodonts, and brachiopods used most commonly (e.g., Trexler Jr. et al., 1996, 2003, 2004). The unconformities are synchronous and are present across much of the northeastern and east-central Nevada (e.g., Trexler Jr. et al., 2003, 2004; Lawton et al., 2017).

The mounting evidence for a transpressional (sinistral) Laurentian margin is based on data of several types. Structural truncation of Paleozoic stratigraphic trends in southeastern California has long been attributed to a sinistral transform margin that formed in the Pennsylvanian (Stone and Stevens, 1988; Walker, 1988). A combination of geologic history, provenance data and paleontological data from Caledonian – Siberian terranes in northwestern Laurentia document southward propagation of a sinistral transform fault system in middle to late

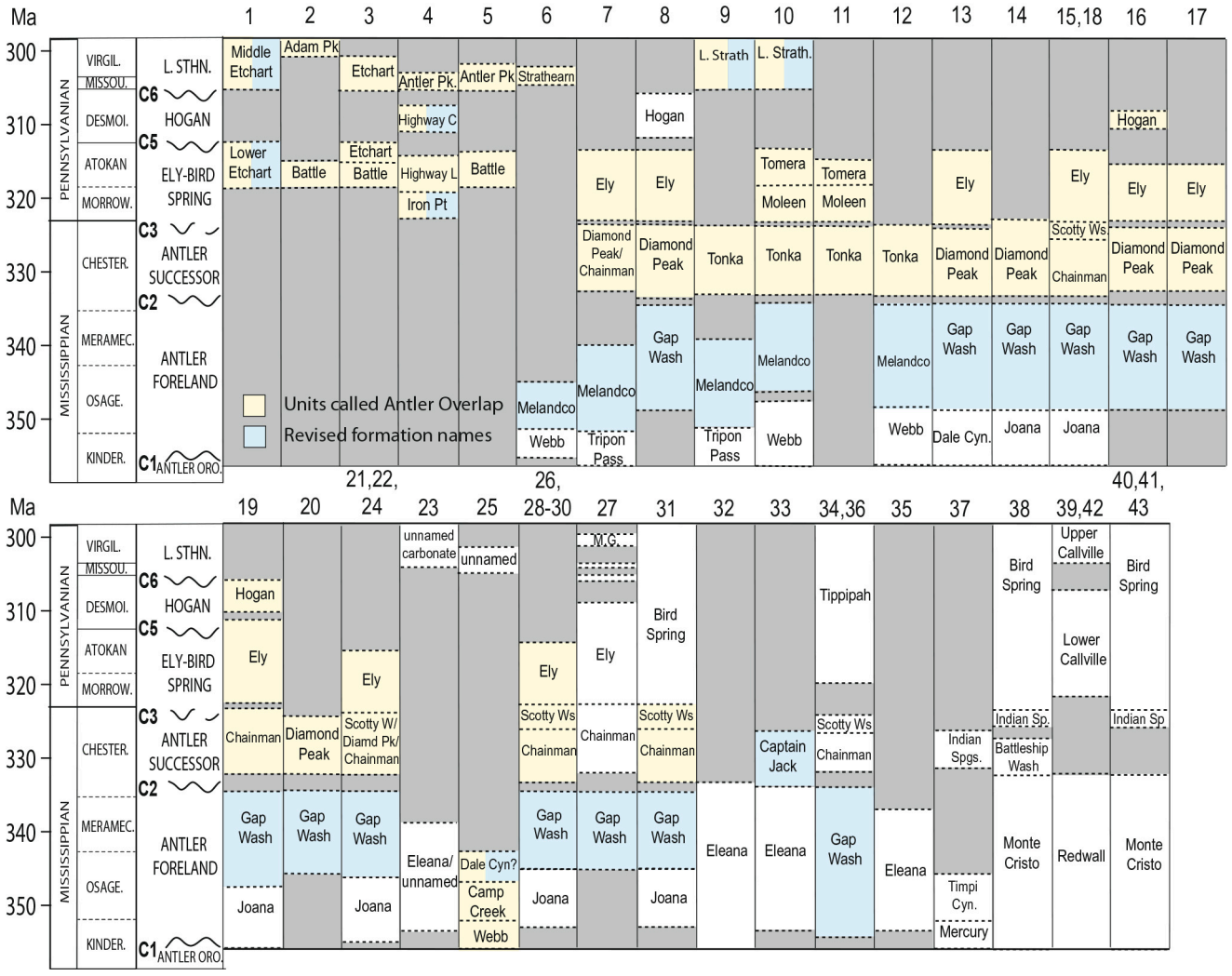


**Fig. 3.** Stratigraphic columns from data control points. Column numbers correspond to locations in Fig. 2. Yellow denotes units included in "Antler Overlap" as defined by Roberts (1964) and/or cited as such in the listed sources. Note they include units *above and below* each of the late Paleozoic unconformities, thus obscuring the evidence for shortening, uplift and erosion at these times. Blue indicates formation names that have been modified based on age and/or position relative to an unconformity. Stratigraphic information is from the following sources (numbers correspond to sections): 1, Dry Hills - Siebenaler (2011); 2, Osgood Mountains, 3, Lone Butte, and 5, Battle Mountain, – Saller and Dickinson (1982); 4, Edna Mountain, – Cashman et al. (2011); 6, Snake Mountains - McFarlane (2001); 7, North Pequop Mountains – Thorman and Brooks (2011); 8, Central Pequop Mountains, – Sweet (2003); 9, Adobe Range, and 10, Carlin Canyon - Trexler Jr. et al., 2004); 11, Grindstone Mountain, Sturmer (2012); 12, Piñon Range – Silberling et al. (1997) and Trexler Jr. et al. (2003); 13, Diamond Mountains - Perry (1994); 14, Maverick Springs Range – Nutt and Hart (2004); 15, Cherry Creek Range – Fritz (1968); 16, Buck Mountain - Whitmore (2011); 17, Butte Mountains – Otto (2008); 18, Schell Creek Range, 21, Pancake Range – Hose et al. (1976); 19, Illipah Reservoir – Crosbie (1997) and Sturmer (2012); 20, Secret Canyon - French and Walker (2018); 22, White Pine Range – Crosbie (1997); 23, Hot Creek Range - McHugh (2006); 24, South Pancake Range, 26, Egan Range – Kleinhampl and Ziony (1985); 25, Monitor Range - Wise (1977); 27, Mountain Home Range - Ritter and Robinson (2009); 28, Grassy Mountains and 29, Fairview Range, Best et al. (1998); 30, Timpahute Range - Russo (2013); 31, Pahranagat Range – Jayko (2007); 32, Eleana Range, 33, Bare Mountain, and 34, Syncline Ridge - Trexler Jr. and Cashman (1997); 35, Shoshone Mountain, 36, CP Hills, and 37, Spotted Range - Trexler Jr. et al. (1996, 2003); 38, Arrow Canyon Range – Bishop et al. (2009, 2010); 39, Virgin Mountains – Rice (1990); 40, Lee Canyon, 41, Las Vegas Range, and 43, Mountain Springs Pass - Page et al. (2005); 42, Frenchman Mountain, Rice (1990) and Castor et al. (2000). See supplemental information for section coordinates. (For interpretation of the references to colour in this figure legend, the reader is referred to the web version of this article.)

Paleozoic time (Colpron and Nelson, 2009). This transform margin evolved into oblique subduction along the entire western margin of Laurentia in Late Devonian time (Nelson et al., 2006; Colpron and Nelson, 2009). Detrital zircon (DZ) provenance data from Nevada are consistent with a sinistral component of offset along the plate boundary. Ordovician rocks in the Roberts Mountains Allochthon (RMA) contain zircon grains derived from a northern Laurentian source (Gehrels and Dickinson, 1995; Gehrels and Pecha, 2014; Linde et al., 2016). Textural characteristics of one zircon-bearing unit suggest that it was tectonically transported southward along the Laurentian margin before its tectonic emplacement in north-central Nevada (Linde et al., 2017). Tectonically driven stratigraphic sequences described in the Copper Basin Group in Idaho document rapid subsidence, unconformities, and depositional changes consistent with intrabasinal deformation (Link et al., 1996). Although attributed to the Antler Orogeny (Link et al., 1996), these features pre-date those in Nevada; this pattern is consistent with southward -propagating tectonism along the plate margin. The northward motion of Laurentia in late Paleozoic time (Cocks and Torsvik, 2011; Domeier and Torsvik, 2014) provides a plate tectonic mechanism for sinistral translation along the margin (Lawton et al., 2017).

## 3. Reconstruction methods

The paleogeographic data are presented for selected late Paleozoic time intervals on a base map reconstructed to Late Pennsylvanian time (~300 Ma; Figs. 2, 4, and 5). We modified a 36 Ma paleogeographic reconstruction by McQuarrie and Wernicke (2005), wherein they restored Basin and Range extension, San Andreas-Walker Lane-Eastern California Shear Zone translation, and metamorphic core complex extension (Fig. 4). Using the 36 Ma maps as a starting point, we restored estimated slip related to the Cretaceous-Paleocene Sevier Orogeny, Jurassic-Cretaceous Central Nevada Fold and Thrust Belt, Western Utah Thrust Belt, the Eastern Sierra Nevada Thrust Belt, and the Permian Last Chance-Belted Range Thrust System (Fig. 5). For each event we restored westward transport of allochthonous material along thrust faults as outlined below. We did not restore the latest Permian Golconda Thrust or the Jurassic Luning-Fencemaker Thrust because they structurally overlie the rocks in this study; allochthon emplacement did not significantly change the position of footwall rocks. We chose not to restore left-lateral(?) slip on the recently identified Getchell-West Fault that was likely active between Middle Pennsylvanian and Permian time. It is part of the major strike-slip fault system that emplaced the Edna Block (see Section 4.3), but the magnitude of slip is currently unknown (Key, 2015; Key and Cashman, 2021). In addition to polygons showing positions of mountain ranges in Nevada and western Utah, these maps also show reconstructed positions of major thrust faults, the initial Sr 0.706 line, and the ranges from which we have data (see supplemental information for section locations). Note that the trace of the "Roberts Mountains Thrust" was taken from published maps, and therefore depicts the present eastern extent of oceanic rocks. It does not necessarily represent a single, continuous fault surface or imply a single age of emplacement.

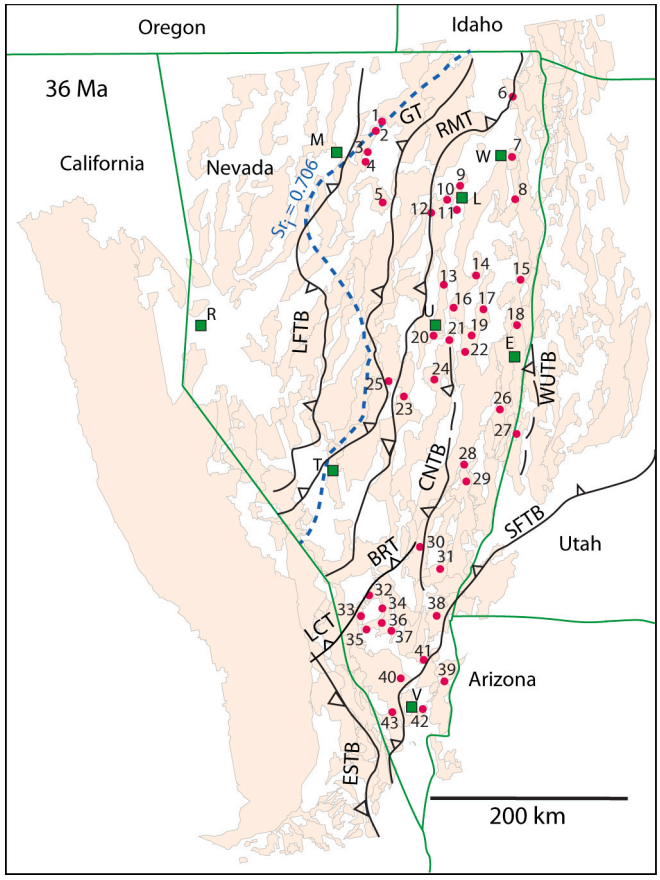


**Fig. 4.** 36 Ma reconstruction of the western Basin and Range with Basin and Range extension and Walker Lane translation restored, modified from McQuarrie and Wernicke (2005) and Long (2015). Data control points are shown by red dots. Numbers correspond to reconstructed section locations shown in Fig. 2 and stratigraphic sections shown in Fig. 3. (For interpretation of the references to colour in this figure legend, the reader is referred to the web version of this article.)

The largest changes to the base map result from restoring slip from the Sevier Orogenic Belt (Fig. 5). Cumulative offsets across the Sevier Orogenic Belt vary from ~240 km in central Utah to ~75 km in southern Nevada (Levy and Christie-Blick, 1989; Currie, 2002; DeCelles, 2004; DeCelles and Coogan, 2006). There is some disagreement with the cumulative shortening in both central Utah and southern Nevada. Levy and Christie-Blick, 1989 interpret 125 km and 135 km cumulative shortening for central Utah and southern Nevada, respectively. More recent work (e.g., Currie, 2002; DeCelles, 2004; DeCelles and Coogan, 2006) requires more than 200 km of cumulative shortening based on more recent reconstructions. For southern Nevada, Levy and Christie-Blick, 1989 include the main Sevier Thrusts (~75 km) and the Last Chance-Belted Range System, which is demonstrably Permian in age (e.g., Snow, 1992; Cole and Cashman, 1999; Snow and Wernicke, 2000; Stevens et al., 2015; Levy et al., 2021). When these are combined, our restoration magnitude is similar to the Levy and Christie-Blick, 1989 estimates. Most of these restorations occur east of the study area, but restorations in the southern Sevier Orogenic Belt greatly modify the facies distributions in the southern portion of the study area (Figs. 4-5). In the southern Nevada section, we restored east-directed motion of 30 km on the Wheeler Pass-Gass Peak Thrust (Burchfiel et al., 1974; Giallorenzo et al., 2018), 7.5 km on the Lee Canyon Thrust (Levy and Christie-Blick, 1989), 5 km on the Deer Canyon Thrust (Levy and Christie-Blick, 1989), and ~ 30 km on the Keystone-Red Springs Thrust (Guth, 1981; Axen, 1984).

Most of the other restorations of Permian to Jurassic deformation involve relatively small-magnitude displacements. The Western Utah Thrust Belt, Central Nevada Fold and Thrust Belt, and Eastern Sierra Thrust Belt all involved restoration of 10–15 km of east-directed transport (e.g., Taylor et al., 2000; Dunne and Walker, 2004; Long, 2015). The Clery-Lemoigne and Marble Canyon-Schwaub Peak-Spectre Range Thrust Systems each had 3 km of east-directed transport restored (Levy and Christie-Blick, 1989). The Last Chance-Grapevine-Belted Range System is a complex system of a shallowly-dipping foreland-vergent thrust paired with a steeply-verging hinterland-vergent thrust (e.g., Snow, 1992; Cole and Cashman, 1999). Estimates for cumulative slip on this system range between 50 and 75 km (e.g., Snow, 1992; Snow and Wernicke, 2000; Stevens et al., 2015; Levy et al., 2021). The cumulative slip appears to decrease northward where the system appears to die out south of Eureka, Nevada (Long, 2012, 2015; Russo, 2013). We restored

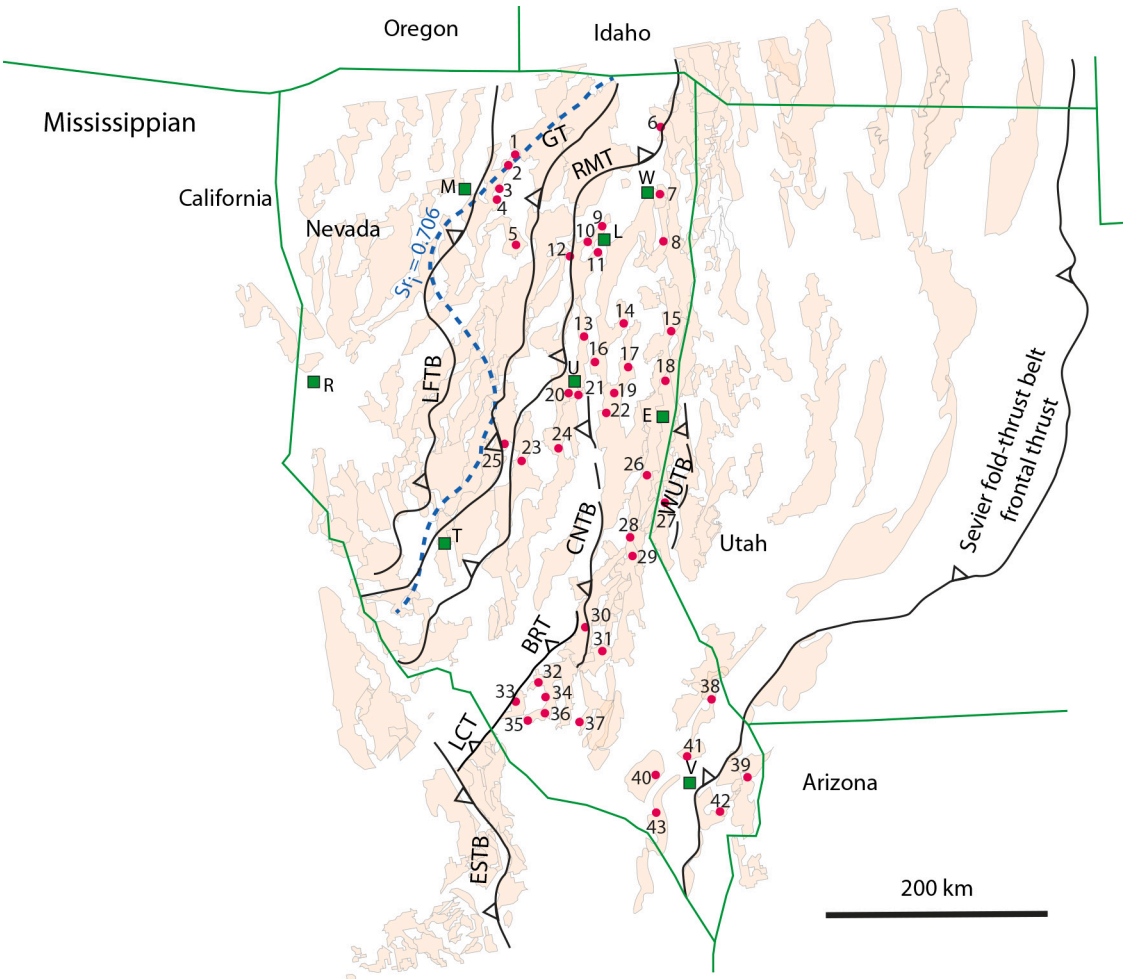


**Fig. 5.** Late Paleozoic reconstruction of the western Basin and Range, modified from the 36 Ma map of McQuarrie and Wernicke (2005) by restoring contractional deformation on Permian, Jurassic, and Cretaceous-Eocene thrust fault systems (this study). Data control points are shown by red dots. Numbers correspond to reconstructed section locations shown in Fig. 2 and stratigraphic sections shown in Fig. 3. (For interpretation of the references to colour in this figure legend, the reader is referred to the web version of this article.)

75 km of east-directed slip on this system, with the amount of slip decreasing toward the north.

Each time slice map contains information about the distribution of depositional environments, paleocurrents, point and clast count data, structures, and spatial extent of unconformities. All data are from a combination of published and unpublished data (Fig. 3). Polygon colors represent approximate bathymetric depositional position from subaerial (yellow) to deep marine (purple). Lithologic pattern overlays show the dominant rock type(s) throughout the area at each time slice (Fig. 6). A combination of unpublished and published paleocurrent data are represented by averaged current arrows over measurement locations with 45-degree sectored rose diagrams shown on the sides of the maps. The types of paleocurrent data shown on each map are specified in the paleogeography descriptions below. Compositional data are shown as a variety of thin section point count and conglomerate clast count ternary diagrams. Several of the maps cover times of localized and/or regional unconformity development. These maps include inferred age range of strata removed at each unconformity, spatial variation in age range of strata removed, and orientation and types of structures that are trimmed by each unconformity.

## 4. Results

### 4.1. Kinderhookian

Initial deposition within the Antler Foreland Basin was dominated by phosphate- and organic-rich mudrocks in the basin depocenter (e.g., Trexler Jr. et al., 1996; French et al., 2020 and references cited therein) with a carbonate shelf forming farther east (e.g., Goebel, 1991) (Fig. 7). Distinctive carbonate turbidites sourced from the craton to the northeast occur in the northernmost part of the basin (e.g., Frye and Giles, 2006). Phosphatic shales extend north-south along length of the study area. A broad carbonate shelf formed to the east; here, limestone with chert nodules transitions southward into oolitic limestone. During this time the Antler Foreland Basin was notably starved of coarse clastic sediment.

A swath of Kinderhookian carbonate turbidite and debris flow strata is exposed across the northern tier of the study area between northwestern Utah and north-central Nevada. This unit, the Tripon Pass Formation, was deposited unconformably atop the Upper Devonian (Frasnian) Guilmette Limestone beginning in middle Kinderhookian time (e.g., Ketner, 1970; Oversby, 1973; Frye and Giles, 2006). The

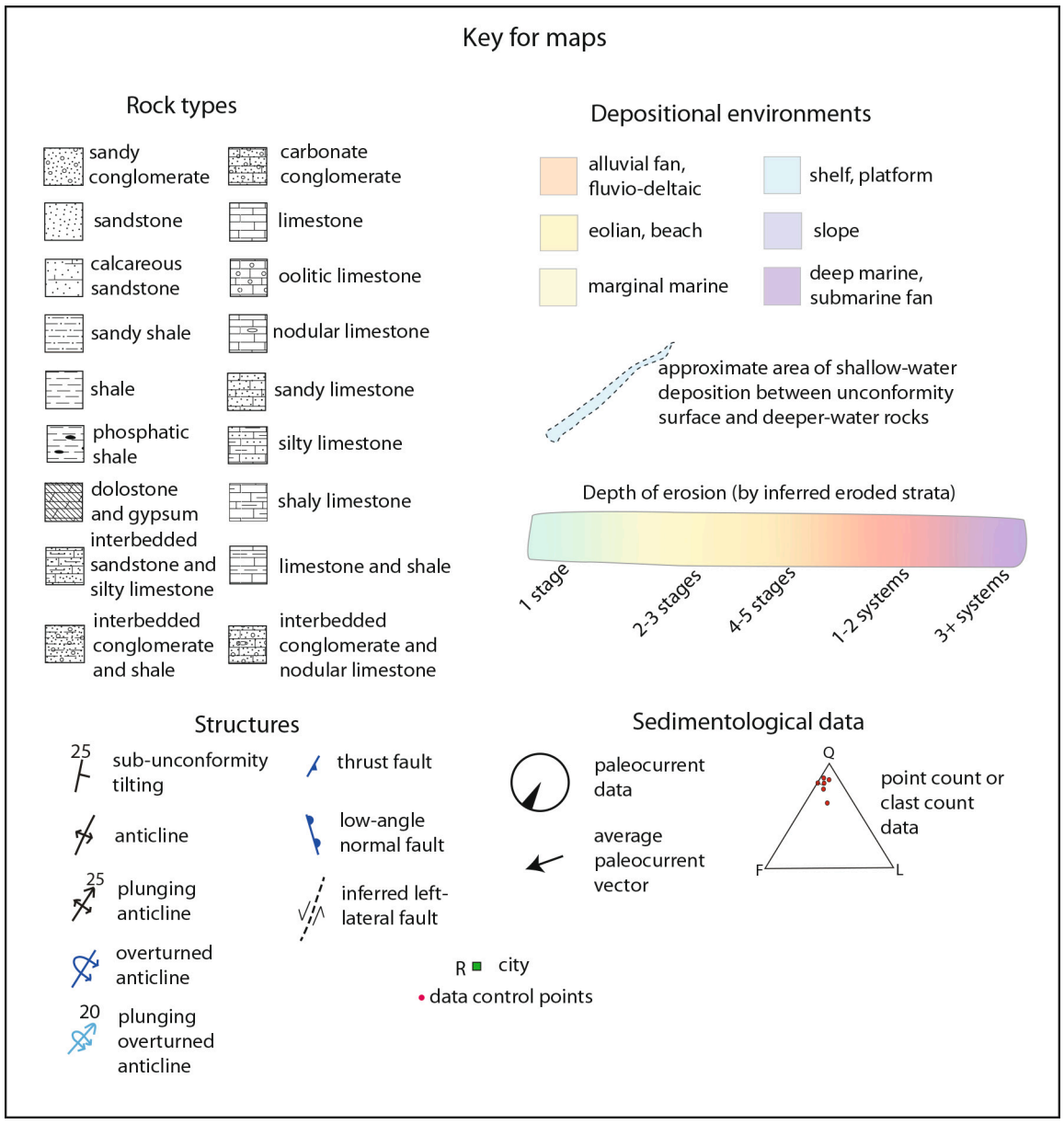


**Fig. 6.** Key for reconstructed time slice maps.

formation is dominated by calcareous siltstone and sandy calcareous siltstone, with carbonate-clast conglomerate and graded carbonate beds occurring in exposures from east of Wells, NV to Elko, NV (Frye and Giles, 2006). Paleocurrent indicators including flute casts suggest flow toward the southwest (Frye and Giles, 2006). This formation is interpreted as a deep marine submarine fan system: the conglomerates and graded beds are turbidites, sourced from the northeast, interbedded with fine-grained hemipelagic material. Frye and Giles (2006) tie distinctive clast types to Frasnian to Kinderhookian units exposed in western and central Utah.

Mudrocks dominate the western portion of the study area. The Webb Formation of northern and central Nevada is dominantly organic-rich argillaceous and calcareous shale and mudstone, locally containing barite nodules (e.g., Smith and Ketner, 1968; Ketner and Smith, 1982; Iverson, 1991). This dark, fine-grained unit is difficult to differentiate from the underlying Upper Devonian Woodruff Formation and from the locally overlying Gap Wash Formation; both are also dark fine-grained units (e.g., Iverson, 1991; French et al., 2020). The Webb Formation has been interpreted as being the distal edges of submarine fans derived from the west and deposited by sediment-gravity flows in a deep marine setting (e.g., Martin, 1985; Iverson, 1991). At the Nevada National Security Site (NNSS) to the south, the Kinderhookian portion of the lower part of the Eleana Formation is a thin section of laminated siltstone and very fine-grained litharenite. These rocks are interpreted as hemipelagic deposits within a system dominated later in Mississippian time by turbidites (e.g., Trexler Jr. and Cashman, 1997).

A carbonate shelf covered the eastern and southern parts of the study area. The Joana Limestone in the northeastern and east-central parts of the study area records a complex carbonate bank. The basal unit is dominated by crinoidal-peloidal packstone, which grades upward into a diverse lithologies including oolitic and crinoidal grainstone, karst breccia, argillaceous wackestone, and fossiliferous mudstone (Goebel, 1991; Giles, 1996). The carbonate complex is interpreted as being deposited primarily in relatively shallow water, ranging from supratidal/intertidal (karst breccia) to lagoonal/shoreface (crinoidal wackestone) to lower ramp (fossiliferous mudstone) (Giles, 1996).

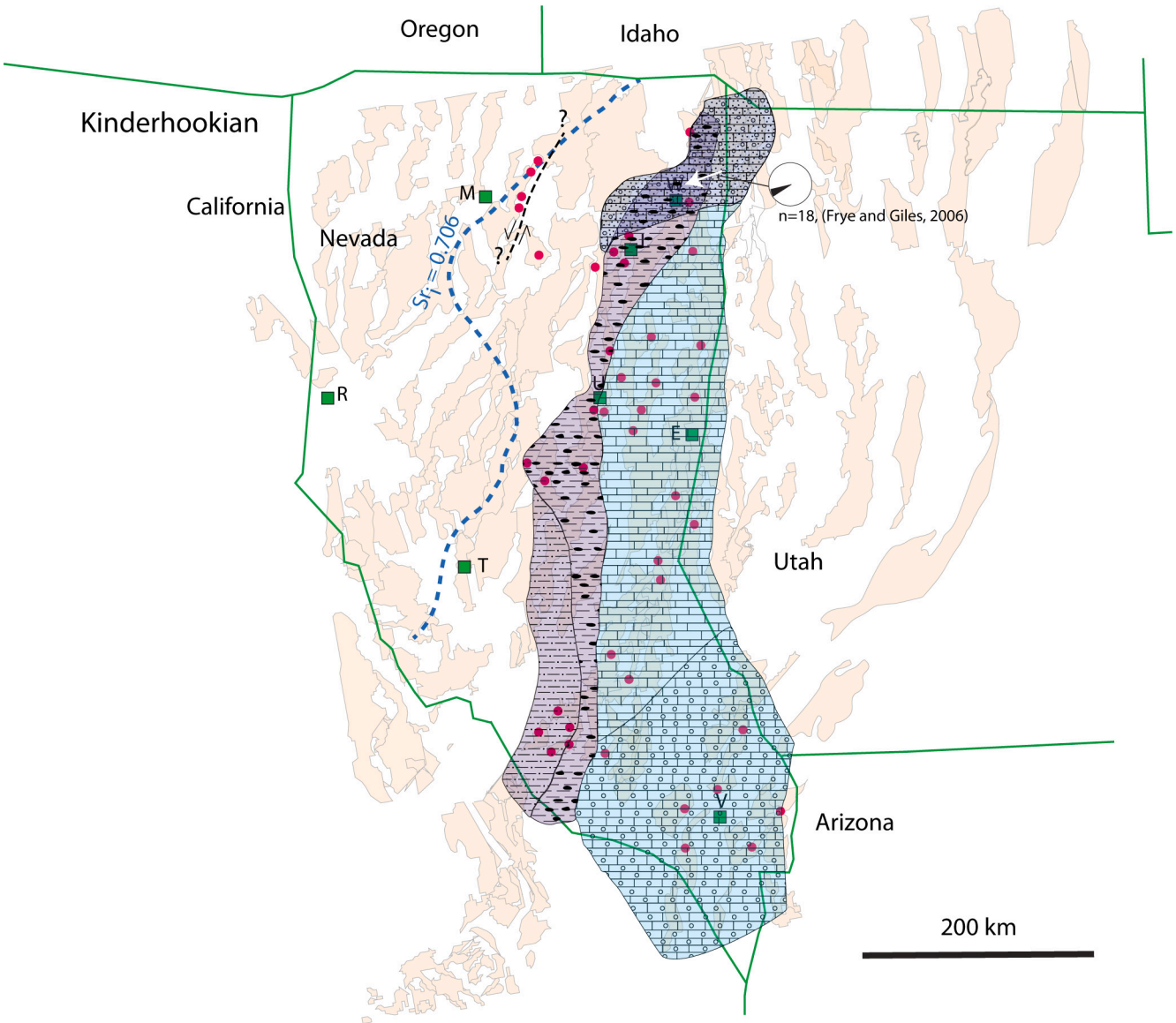


**Fig. 7.** Paleogeographic map for Kinderhookian time on the late Paleozoic reconstructed base map (Fig. 5). Map shows estimated minimum extents of depositional belts (patterned). Extent of data to the west for this and all maps is controlled by a lack of exposure of late Paleozoic strata. Paleocurrent data from Frye and Giles (2006). E, Ely; L, Elko; M, Winnemucca; R, Reno; T, Tonopah; U, Eureka; V, Las Vegas; W, Wells.

Kinderhookian units in southern Nevada are dominantly crinoidal and oolitic packstone and grainstone (e.g., Langenheim Jr. et al., 1962; Page et al., 2005).

The Antler Foreland Basin was starved of coarse clastic sediment during Kinderhookian time. Initial deposition within the Antler foredeep was almost exclusively fine-grained. Although initial fine-grained deposition that has been tied to the Antler Orogeny began in latest Devonian time, coarse clastic sediment did not arrive in the Antler Foreland Basin until Osagean time, more than 10 Myr later (Trexler Jr. and Cashman, 1997). The delay in coarse clastic arrival into the foreland basin may be related to the general marine highstand in Early Mississippian time (e.g., Trexler Jr. and Cashman, 1997), or to the Antler Orogenic Belt being relatively distant or topographically low during Kinderhookian time. In contrast, Kinderhookian submarine fan strata in Idaho are several times thicker than those in Nevada (Link et al., 1996).

### 4.2. Osagean

Coarse-grained siliciclastic turbidites first arrived in the Antler Foreland Basin in Osagean time (Trexler Jr. et al., 2003, and references therein). The turbidity currents flowed south, along the axis of the foreland basin and parallel to the continental margin (Fig. 8). The basin fill is thickest and coarsest to the west, consistent with a northwestern source, and grades eastward into an organic-rich, mudstone-dominated section. The carbonate shelf bordered the foreland basin on the east. These conditions prevailed throughout Osagean and Meramecian time, until deposition in the Antler Foreland Basin was terminated by shortening and uplift in late Meramecian – early Chesterian time.

The composition of the coarse-grained foreland basin deposits varies with location and stratigraphic position, elucidating the paleogeography of the basin. The rocks represent fan lobes and channels in the submarine

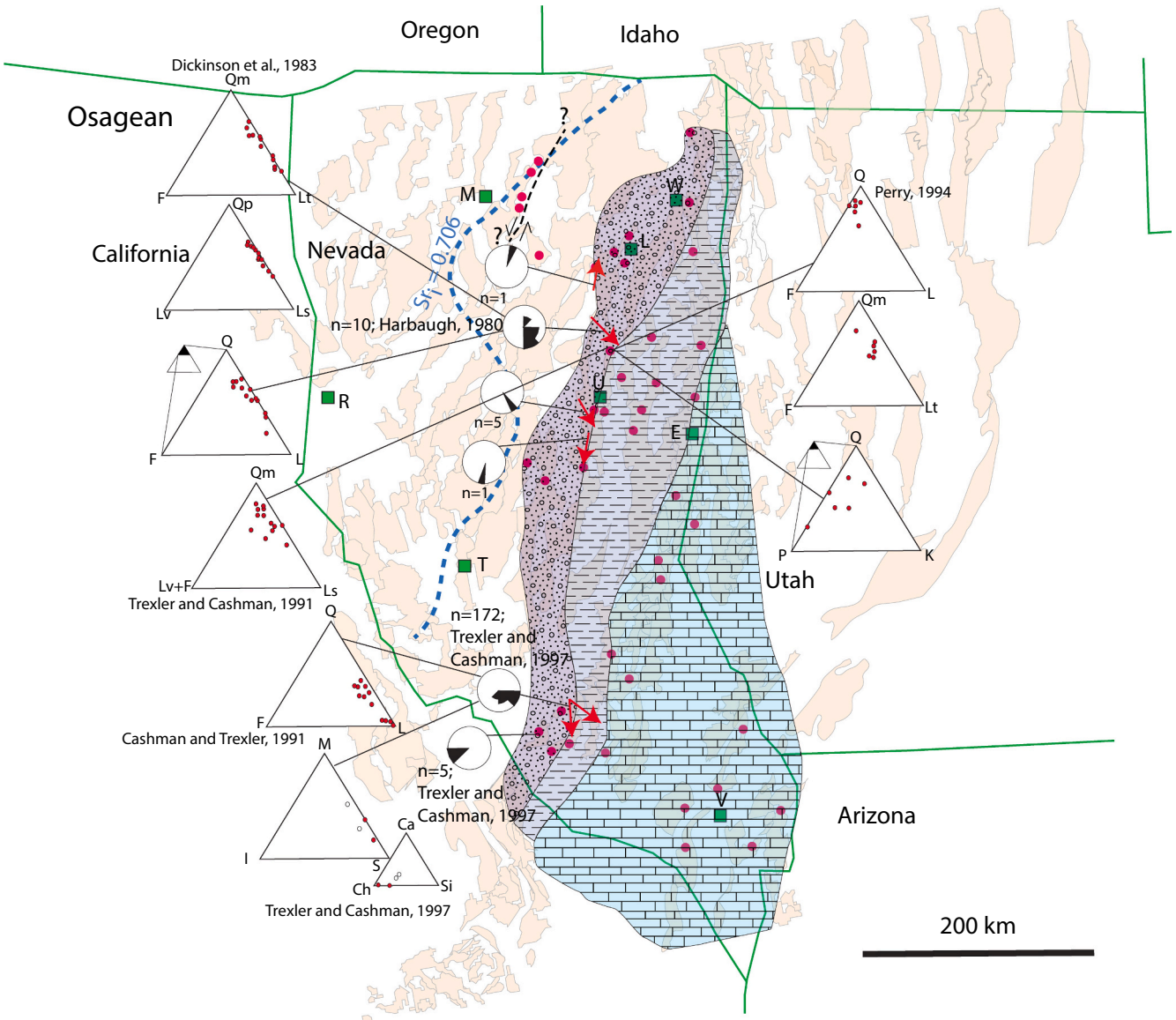


**Fig. 8.** Paleogeographic map for Osagean time on the late Paleozoic reconstructed base map (Fig. 5). Maps show estimated minimum extents of depositional belts (patterned). Paleocurrent data from Harbaugh (1980) and Trexler Jr. and Cashman (1997). Compositional data from Dickinson et al. (1983), Cashman and Trexler Jr. (1991), Trexler Jr. and Cashman (1991, 1997), and Perry (1994). E, Ely; L, Elko; M, Winnemucca; R, Reno; T, Tonopah; U, Eureka; V, Las Vegas; W, Wells.

fan. Conglomerates are overwhelmingly composed of resistant clasts, dominantly chert and quartzite (e.g., Dott Jr., 1955; Harbaugh, 1980). Less abundant clasts include argillite, litharenite, lithic wacke, recrystallized limestone, and siltstone (e.g., Trexler Jr. and Cashman, 1991, 1997; Trexler Jr. et al., 2003; and references therein). Distinctive heterolithic conglomerates containing limestone and volcanic clasts occur low in the section in the Diamond Mountains (Fig. 2, #13) (Brew and Gordon Jr., 1971) and in the Eleana Range (Fig. 2, #32) (Trexler Jr. and Cashman, 1997). These less resistant heterolithic clasts do not occur higher in the section. The Eleana Range exposures indicate two sediment sources for this part of the basin: the turbidites containing limestone and volcanic clasts have SE-directed paleocurrent indicators; they are interbedded with the more common S-directed siliciclastic turbidites (Trexler Jr. and Cashman, 1997) (Fig. 8). Sandstones are primarily litharenites and quartz arenites; the relative percentages of quartz and chert grains vary with location. Less common grains include quartzite, sedimentary lithics, volcanic lithics, and feldspar (e.g., Dott Jr., 1955; Harbaugh, 1980; Trexler Jr. and Cashman, 1991). The quartz-rich sediments could be derived from the craton or the Antler Allochthon. However, the only regionally significant source of radiolarian chert clasts is the Valmy and Vinini formations of the Antler Allochthon (e.g., Dickinson et al., 1983).

Mudrocks include finely laminated siliceous siltstone, argillite, and shale with local fine-grained sandstone beds. They comprise both distal and interlobe deposits on the submarine fan. Plant debris (locally current-oriented) and trace fossils are found locally on bedding planes (e.g., Poole, 1974; Harbaugh, 1980; Trexler Jr. and Nitchman, 1990; Trexler Jr. and Cashman, 1991). The trace fossils indicate quiet, but well-aerated, marine conditions. However, in much of the mudrock section, abundant organic matter and associated uranium record deposition in a reducing environment (French et al., 2020). This mudstone has been identified in wireline logs for 153 wells in Nevada and westernmost Utah, so its distribution, thickness, and mineralogic and petrophysical characteristics are well documented (French et al., 2020). Microfossil collections identified by B. Mamet indicate an Osagean through middle Meramecian age for these rocks in both central and southern Nevada (1989, written commun., in Trexler Jr. and Cashman, 1991; see also extensive biostratigraphic summaries in Trexler Jr. et al.,

1996).

Stacked thrust sheets at NNSS and Bare Mountain (Fig. 2, #32–37) preserve the southern and southwestern parts of the Middle Mississippian submarine fan in southern Nevada. First, they provide unequivocal documentation of sand provenance: sand and silt grains in mudstone of the autochthonous Gap Wash Formation are primarily monocrystalline quartz, while those in argillite of the allochthonous Eleana Formation are dominantly chert (Trexler Jr. and Cashman, 1997). Second, where thrust faults duplicate siliciclastic turbidite sections, the upper plate (derived from farther to the west) contains facies deposited in a more source-proximal position on the fan (Trexler Jr. and Cashman, 1997). Third, phosphatic clasts occur in the structurally highest thrust plate. Rare to absent elsewhere, they were most likely derived from chert with phosphatic nodules common in some parts of the Antler Allochthon (Trexler Jr. and Cashman, 1997).

The carbonate platform and marginal shelf persisted in east-central and southern Nevada throughout Osagean – Meramecian time. In southern Nevada, this includes the upper Dawn Limestone, Anchor Limestone, and Bullion Limestone members of the Monte Cristo Group (Hewett, 1931; Stevens et al., 1996; Page et al., 2005). The Dawn Limestone contains fossiliferous peloidal packstone and wackestone with corals, brachiopods, bryozoans, and crinoid ossicles (Stevens et al., 1996). The Anchor Limestone tends to be thinner-bedded mudstone and wackestone with abundant chert nodules and layers and minimal fossils (Stevens et al., 1991, 1996). The Bullion Limestone is crinoid-rich packstone and grainstone which is locally completely dolomitized (Stevens et al., 1996). The Dawn and Bullion limestones have been interpreted as a shallow-water carbonate platform, whereas the Anchor Limestone represents a deepening to near or below storm-wave base (Stevens et al., 1996). The deeper Anchor Limestone facies are likely related to a positive sea-level excursion during early Osagean time, with sea-level drawdown and shelf progradation leading to shallowing

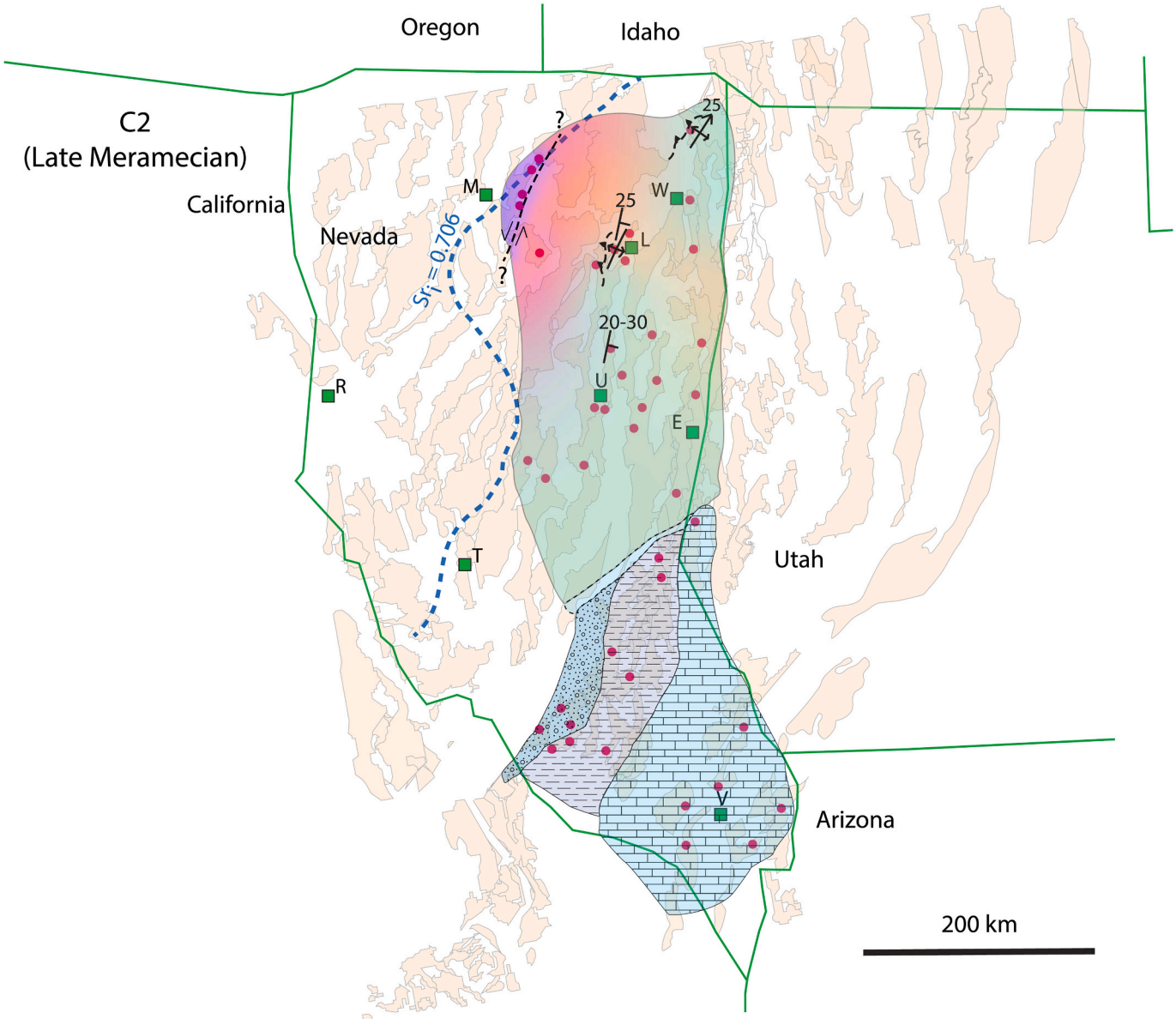


**Fig. 9.** Paleogeographic map for C2 unconformity (late Meramecian) on the late Paleozoic reconstructed base map (Fig. 5). Maps show estimated minimum extents of depositional belts (patterned). Structure symbols show general orientation and style of deformation preserved in strata below the unconformity (McFarlane, 1997, 2001; Trexler Jr. et al., 2003). Color ramp represents depth of erosion inferred from age of unit below the unconformity (see Fig. 6). Light blue represents area of inferred shallow-water deposition between deep marine deposition and subaerial exposure. E, Ely; L, Elko; M, Winnemucca; R, Reno; T, Tonopah; U, Eureka; V, Las Vegas; W, Wells. (For interpretation of the references to colour in this figure legend, the reader is referred to the web version of this article.)

throughout Osagean time (Fig. 8, Stevens et al., 1996).

### 4.3. C2 unconformity surface

The C2 unconformity formed during late Meramecian – early Chesterian time and records tectonic shortening, uplift, and subaerial exposure across northern and central Nevada, while marine deposition continued to the south (Fig. 9). The southern boundary of the C2 unconformity surface (i.e., the paleo-shoreline) trends NE, consistent with maximum uplift to the northwest. This unconformity surface separates the submarine fan and organic-rich shale deposits of the Antler Foreland Basin from the overlying fluvio-deltaic and black shale deposits of the Antler Successor Basin. Both the areal distribution and the erosional depth of the unconformity indicate that the associated tectonic uplift was greatest to the north and west (Fig. 9). Structures below the unconformity record W-E or NW-SE shortening, and eastward vergence. In some (tectonically displaced) northwestern localities (Fig. 2, #1–4), erosion of the tectonic highland removed the entire RMA and much of the underlying autochthonous lower Paleozoic section. In contrast to the northern and central parts of the state, there is no C2 unconformity in southern Nevada. Although marine conditions persisted during Meramecian - early Chesterian time, earliest Chesterian sediments document an abrupt change in provenance and depositional environment.

Structures truncated by the C2 unconformity record the style, geometry, and kinematics of the late Middle Mississippian tectonic event. Angular bedding relationships along the C2 unconformity at Carlin Canyon, the Adobe Range, the Diamond Mountains and the Piñon Range (Fig. 2, #9, 10, 12, 13) cut down-section westward, consistent with tectonic uplift to the west (e.g., Silberling et al., 1997; Trexler Jr. et al., 2003, 2004, and references therein). Structures below the unconformity include east- or southeast-vergent folds, east- or southeast-directed thrust faults, and locally complex imbricate thrust stacks (McFarlane, 1997, 2001; Silberling et al., 1997; Trexler Jr. et al., 2003, and references therein). Particularly notable, because of both its complexity and its location in far northeastern Nevada, is the structure in the northern Snake Mountains (Fig. 2, #6). There, the major stratigraphic units of the RMA are duplicated and structurally interleaved with rocks of the Antler Foreland Basin. Structures include foreland-dipping imbrications, and an antiformal thrust stack documenting top-to-the-southeast tectonic transport; folds in autochthonous footwall rocks plunge northeast (McFarlane, 1997, 2001).

The northwesternmost localities in this study (Fig. 2, #1–4) were anomalously deeply eroded, thus recording substantial tectonic uplift during and following C2 time. Encompassing Edna Mountain, Lone Butte, Dry Hills, and the Osgood Mountains, these localities will herein be referred to as the Edna Block. Erosion of the tectonic highland at these localities removed the entire RMA and the underlying autochthonous lower Paleozoic section, so, at three of them, Lower Pennsylvanian sediments were deposited on Cambrian rocks (e.g., Ferguson et al., 1952; Hotz and Willden, 1964; Erickson and Marsh, 1974a, 1974b, 1974c; Saller and Dickinson, 1982; Villa, 2007; Cashman et al., 2011). Tectonic unroofing along a low-angle normal fault at Edna Mountain (Fig. 2, #4) is additional evidence of extreme tectonic shortening and uplift (Villa, 2007; Cashman et al., 2011, and references therein). In contrast, Lower Pennsylvanian sedimentary rocks at Battle Mountain, the next closest late Paleozoic rocks to the east (Fig. 2, #5) overlie the Harmony Formation, which is structurally high in the RMA (Saller and Dickinson, 1982).

Field relationships at Edna Mountain (Fig. 2, #4) further constrain this contrast in erosional depth, and require at least one high-angle fault with substantial lateral offset between Edna Mountain and Battle Mountain. On most of Edna Mountain, Lower Pennsylvanian rocks overlie Cambrian rocks. Detrital zircon (DZ) studies indicate that the Upper Precambrian-Cambrian section is not exotic to North America; the rocks are correlative to contemporaneous passive margin strata in western Laurentia (Linde et al., 2014). Therefore, the RMA and most of the autochthonous Paleozoic section was eroded here, exposing Cambrian rocks at the ground surface in Early Pennsylvanian time (Erickson and Marsh, 1974a, 1974b, 1974c; Saller and Dickinson, 1982; Villa, 2007; Cashman et al., 2011). In startling contrast, strata on the east side of Edna Mountain are Ordovician, and correlate with the autochthonous section farther east (Key, 2015; Key and Cashman, 2021). This stratigraphic mismatch requires a fault with significant lateral offset. At present, these contrasting sections at Edna Mountain are separated by a NW-striking, SW-dipping fault (Erickson and Marsh, 1974a; Key, 2015; Key and Cashman, 2021). Counterclockwise rotation of structures at Edna Mountain relative to synchronous structures elsewhere in northern Nevada is consistent with sinistral slip (Key and Cashman, 2021). So although any original kinematic indicators on the fault surface have been overprinted by later structures, it is interpreted to be a sinistral transpressive fault (Key and Cashman, 2021).

Although sedimentation was continuous during Meramecian-Chesterian time in southern Nevada, there was an early Chesterian change in both depositional setting and sediment composition of the allochthonous rocks in the higher thrust sheets at the NNSS (Trexler Jr. and Cashman, 1997). Sedimentation continued unchanged in the carbonate platform to the east, and in the adjacent muddy marginal shelf (Trexler Jr. et al., 1996) (Fig. 9). In the southern end of the Antler Foreland Basin, however, earliest Chesterian time was marked by an abrupt change from siliciclastic turbidites to carbonate turbidites (Trexler Jr. and Cashman, 1997). A disconformity in the Spotted Range (Fig. 2, #37) records local subaerial exposure at the margin of the carbonate shelf, likely related to persistent sea level drawdown during the Late Mississippian (e.g., Bishop et al., 2010).

### 4.4. Early Chesterian

In early Chesterian time, sediments of the Antler Successor Basin buried the C2 unconformity in northern Nevada (Fig. 10). A pulse of coarse-grained fluvial-deltaic sediment prograded into the basin from the tectonic highland to the northwest. These fluvial-deltaic sediments built eastward and southward, interfingering with marine limestone locally, and grading into mudrock that makes up much of the Antler Successor Basin. Submarine fan deposition continued west of the muddy marginal shelf in southern Nevada, but the sediment was finer grained than it was earlier in the Mississippian, and the dominant composition changed from siliciclastic turbidites to allodapic limestone turbidites and spiculite. These record deeper and quieter conditions as well as a change in sediment source. To the east, cross-stratified grainstone and microbialite deposited in a tidal flat environment grade southward into an exposure surface.

Sedimentologic studies document the paleogeography and evolution of the Antler Successor Basin. Exposures in the Diamond Mountains (Fig. 2, #13) record a range of fluvial, deltaic, and shallow marine environments (e.g., Harbaugh, 1980; Perry, 1994). Paleocurrents were dominantly toward the southeast. Fluvial deposits thin southward, and the interfingering shallow marine deposits thin northward, recording two siliciclastic progradations and three marine carbonate transgressions in all (Perry, 1994). In the White Pine Mountains farther southeast (Fig. 2, #22), the rocks are dominantly shale (Crosbie, 1997). Siltstone, sandstone, and carbonate beds interbedded with the shale are thin and laterally extensive. Thick or coarser-grained beds are present, but rare. Bioturbation is present, but not common. These rocks represent a distal prodelta to basinal depositional environment (Crosbie, 1997).

In contrast to the heterolithic and matrix-rich rocks of the Antler Foreland Basin, the coarse-grained deposits of the successor basin are clean, chert-quartzite-lithic conglomerate and sandstone with interbedded calcareous litharenite. The conglomerate clast petrology of the fluvial-deltaic deposits includes recycled clasts eroded from the Antler Foreland Basin, so documents a source in the RMA; chert and quartzite clasts dominate (e.g., Dott Jr., 1955; Harbaugh, 1980; Trexler Jr. and Cashman, 1991; Perry, 1994; Crosbie, 1997; and references therein)

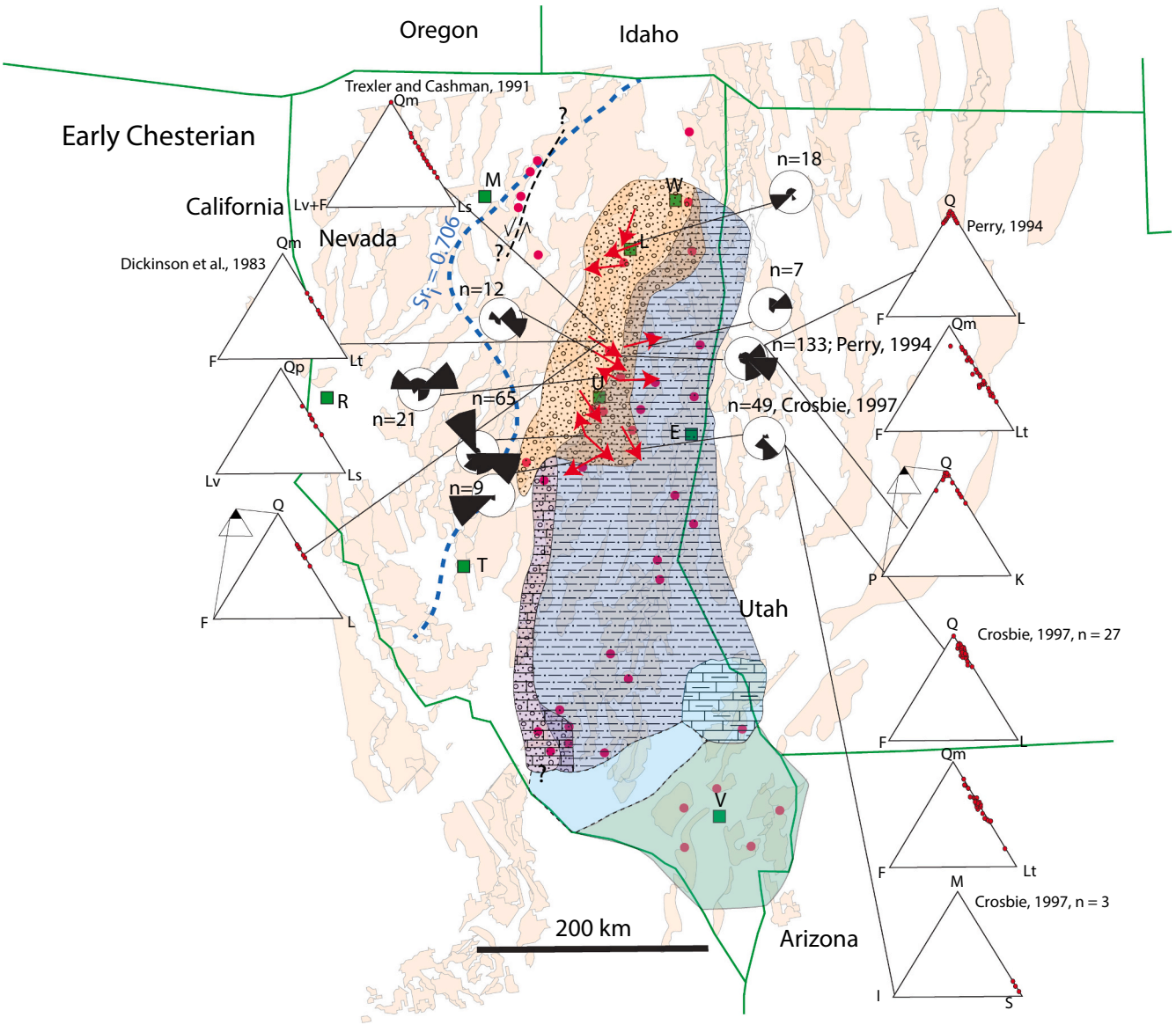


**Fig. 10.** Paleogeographic map for early Chesterian time on the late Paleozoic reconstructed base map (Fig. 5). Maps show estimated minimum extents of depositional belts (patterned). Light blue represents area of inferred shallow-water deposition between deep marine deposition and subaerial exposure. Southern light green area represents a local unconformity. Paleocurrent data from Perry (1994), Crosbie (1997), and unpublished data from Trexler Jr. Compositional data from Dickinson et al. (1983), Trexler Jr. and Cashman (1991), Perry (1994), and Crosbie (1997). E, Ely; L, Elko; M, Winnemucca; R, Reno; T, Tonopah; U, Eureka; V, Las Vegas; W, Wells. (For interpretation of the references to colour in this figure legend, the reader is referred to the web version of this article.)

(Fig. 10). Sandstones contain monocrystalline quartz and sedimentary lithics (including chert); there are notably fewer volcanic lithics and feldspar grains than in sandstones of the underlying Antler Foreland Basin (e.g., Harbaugh, 1980; Trexler Jr. and Cashman, 1991; Perry, 1994; Crosbie, 1997) (Fig. 10). Analysis of ternary diagrams using the model of Dickinson et al. (1983) suggests both recycled orogen and cratonic interior sediment sources for the sandstones of the Antler Successor Basin (e.g., Perry, 1994). Sandstones in the more distal deposits of the White Pine Range are compositionally mature to supermature, containing 95–99% monocrystalline quartz. The most likely source for this quartz is the craton to the east (Crosbie, 1997).

Mudrocks of the Antler Successor Basin are distinct from those of the underlying Antler Foreland Basin; the two can be distinguished in both surface exposures and the subsurface (French et al., 2020): Antler Successor Basin mudrocks have been identified in 151 wells in Nevada, 54 of which contain both foreland basin and successor basin mudrocks. They are significantly higher in clay, lower in quartz, and lower in organic carbon content than those of the Antler Foreland Basin. This suggests that the Antler Successor Basin was shallower or had better circulation. The thicknesses and lateral extents of the two mudrock units are similar, but the lateral limits and depocenter of the Antler Successor Basin are slightly farther east (French et al., 2020).

Stacked thrust sheets at NNSS and Bare Mountain (Fig. 2, # 32–37) record the evolving submarine fan system to the west. Although the Mississippian submarine fan section fines upward overall, it changes abruptly in early Chesterian time from siliciclastic turbidites derived from the north and northwest to carbonate turbidites derived from a productive carbonate platform, probably to the east or southeast (Fig. 10) (Trexler Jr. and Cashman, 1997). In the lower (eastern) plate, the arrival of allodapic limestone coincides with a change to hemipelagic sedimentation. It contains thicker and coarser limestone turbidites than the farther-traveled upper plate. Sedimentation in the upper (western) plate changes from coarse siliciclastic turbidites to argillite and spiculitic chert, with thin beds of chert litharenite and graded

allodapic limestone. The presence of more spiculite and fewer grainstone turbidites in this upper plate indicates that it was farther from the source of limestone detritus than the eastern thrust sheet. The chert pebbles in the allodapic limestone of both thrust sheets are recycled; they were most likely derived from the slightly older Antler foredeep strata (Trexler Jr. and Cashman, 1991, 1997). The thinner section of submarine fan strata at the Bare Mountain area (Fig. 2, # 32) suggests that the submarine fan section may not have extended much farther to the southwest than this area (Trexler Jr. and Cashman, 1997).

To the east, karsted coarse-grained carbonates grade southward into an unconformity surface. At Arrow Canyon (Fig. 2, #38), the late Meramecian - early Chesterian Battleship Wash Formation contains a basal unit of Meramecian photozoan carbonates overlain by Chesterian cross-bedded crinoidal grainstone (Bishop et al., 2009). The upper unit also contains dolomudstone with fenestral fabric, peloid packstone and grainstone, and thrombolites (Bishop et al., 2009). The upper surface of the Battleship Wash is a major karst surface with large potholes and dissolution fractures. The most conspicuous features on the karst surface are meter-scale radiating *Stigmaria* rhizoliths, which are remnant root systems of lycopsid trees (Pfefferkorn, 1972; Phillips and DiMichele, 1992; Clapham and Bishop, 2010). The upper part of the unit is interpreted as deposits of a humid tidal flat (Bishop et al., 2009). The karstification likely resulted from a sea-level drawdown during a major glacial expansion in the Late Mississippian (Bishop et al., 2010). A relatively short-lived hiatus is represented by a disconformity between the top of the lower Chesterian Battleship Wash Formation and the overlying upper Chesterian Indian Springs Formation (Lane et al., 1999; Bishop et al., 2009). Farther south, the Battleship Wash Formation is not present and the depositional hiatus was longer lived, with Indian Springs Formation deposited on Meramecian Yellowpine Limestone (e.g., Page et al., 2005; Sturmer, 2012).

### 4.5. Late Chesterian

The late Chesterian drop in sea level triggered dramatic changes in depositional environments in the Antler Successor Basin (Fig. 11).

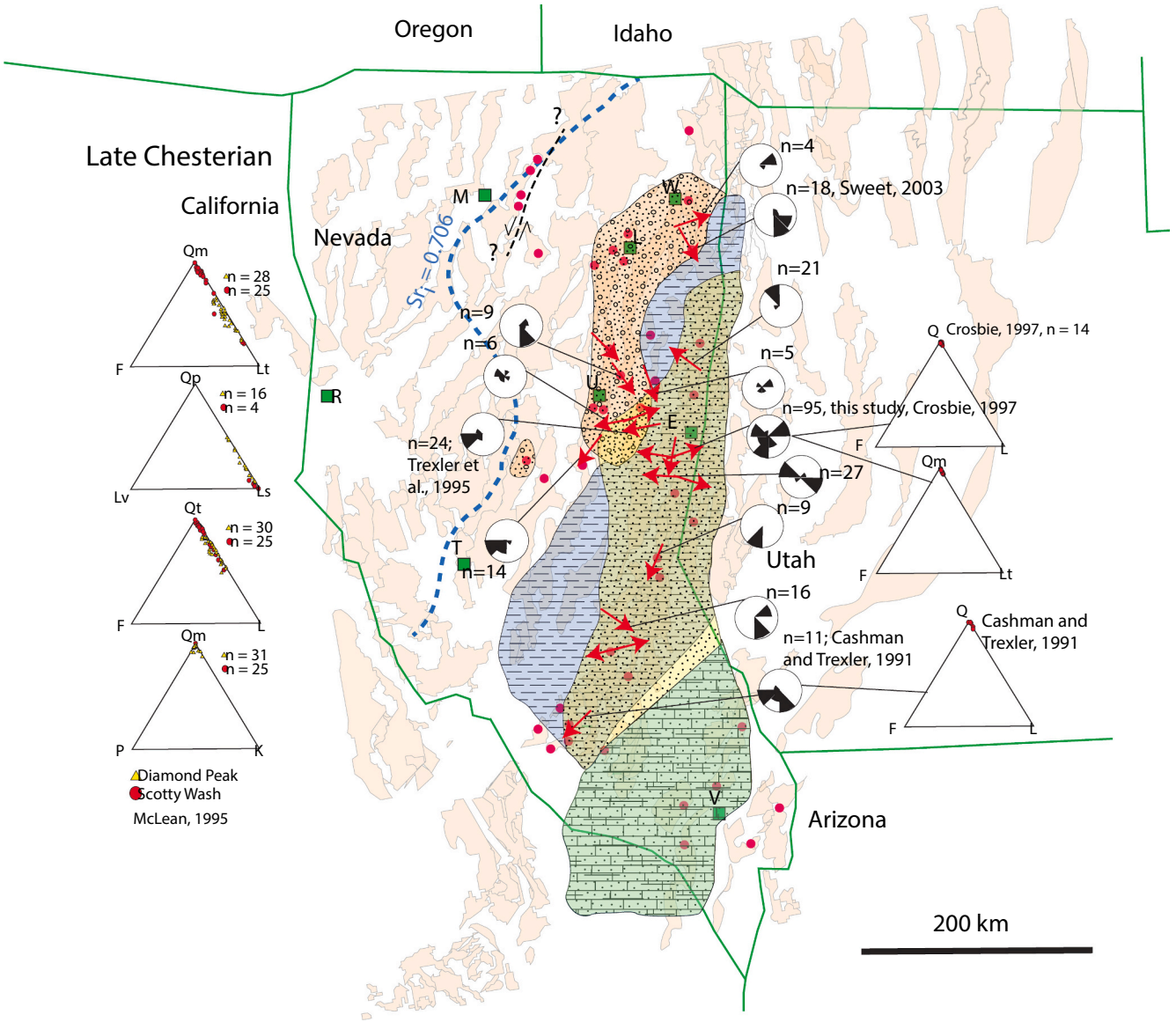


**Fig. 11.** Paleogeographic map for late Chesterian time on the late Paleozoic reconstructed base map (Fig. 5). Maps show estimated minimum extents of depositional belts (patterned). Paleocurrent data from Cashman and Trexler Jr. (1991), Trexler Jr. et al. (1995), Crosbie (1997), Sweet (2003), and unpublished data from Trexler Jr. Compositional data from Cashman and Trexler Jr. (1991), McLean (1995), and Crosbie (1997). E, Ely; L, Elko; M, Winnemucca; R, Reno; T, Tonopah; U, Eureka; V, Las Vegas; W, Wells.

Coarse-grained clastic sediments continued to enter the basin from the northwest. Farther east, deposition of distal mudrocks continued. Continent-derived quartz arenite prograded west and south into the basin and was transported southwest along the continental margin. The quartz arenite interfingers with the distal mudrocks and locally even interfingers with coarser-grained sediment derived from west of the basin. Elsewhere, the carbonate shelf was replaced by a broad nearshore marine and coastal swamp environment. Note that no Antler Successor Basin sediments are preserved at the northwesternmost localities in this study (Fig. 2, #1–5), suggesting that erosion, and possibly tectonic uplift, continued there throughout Chesterian time.

The coarse-grained strata in the northwestern part of the basin are continuous with, and indistinguishable from, the lower Chesterian deposits. They are compositionally and texturally mature. Conglomerate clasts are dominantly chert and quartzite; sandstone grains are dominantly chert and quartz. Both indicate recycling from sources in the RMA. Conglomerate units in the White Pine Range (Fig. 2, #22) record delta braid-plain, shoreface and marginal marine environments (Crosbie, 1997). Paleocurrent directions in these rocks are generally toward the southeast (Fig. 11). Near the southern limit of the coarse-grained deposits, they are interbedded with craton-derived quartz arenites with southwest-directed paleocurrent indicators (note overlapping composition patterns on Fig. 11).

The finer-grained deposits on the eastern flank of the basin record a variety of environments. Shale and mudstone record deeper water conditions. In the White Pine Range (Fig. 2, #22), the lower Chesterian prodelta deposits are overlain by and interfinger with well-sorted quartz arenite recording nearshore beach and offshore bar environments (Crosbie, 1997). Paleocurrents from these quartz arenites document a strong south- to southwesterly flow (Fig. 11). Abundant shale and minor mudstone also occur in this section, and represent quiet, relatively deep deposition.

Farther south, interbedded paleosols and fossiliferous shallow marine limestones dominate the stratigraphy (Fig. 11). These rocks were deposited disconformably atop Meramecian limestone or lower Chesterian karsted limestone with *Stigmaria* rhizomorph systems (Bishop et al., 2009; Clapham and Bishop, 2010). Limestone beds tend to be fossiliferous, dominated by large productid brachiopods, including *Flexaria, Inflatia,* and *Diaphragmus* (Webster and Lane, 1967; Clapham and Bishop, 2010). Other brachiopods, and echinoderms are also locally abundant (Lane, 1964; Webster and Lane, 1970; Brenckle et al., 1997). These strata are consistent with deposition in a marginal marine depositional environment with relatively high-amplitude (<60 m) sea level change (Clapham and Bishop, 2010). Paleosols include a combination of vertisols, argillisols, and protosols, consistent with a sub-humid to subarid climate with high seasonality (Bishop et al., 2009; Clapham and Bishop, 2010).

Autochthonous rocks in the southwesternmost localities (Fig. 2, # 34–36) are shale and sandstone of the marginal shelf (Trexler Jr. et al., 1996). At Mine Mountain (Fig. 2, # 35), the shale contains distinct beds of chert litharenite and quartz arenite, evidence of interfingered allochthon-derived and craton-derived sands, respectively (Fig. 11). Bimodal paleocurrent indicators in quartz arenite bar sands near Syncline Ridge suggest tidal influence. The amount of mature, craton-derived quartz sand increases near the top of these sections (Trexler Jr. et al., 1996), and extends into strata of Morrowan age at Syncline Ridge (Fig. 2, # 34) (Titus, 1992; Titus and Manger, 1992).

No upper Chesterian rocks are preserved in the southwestern

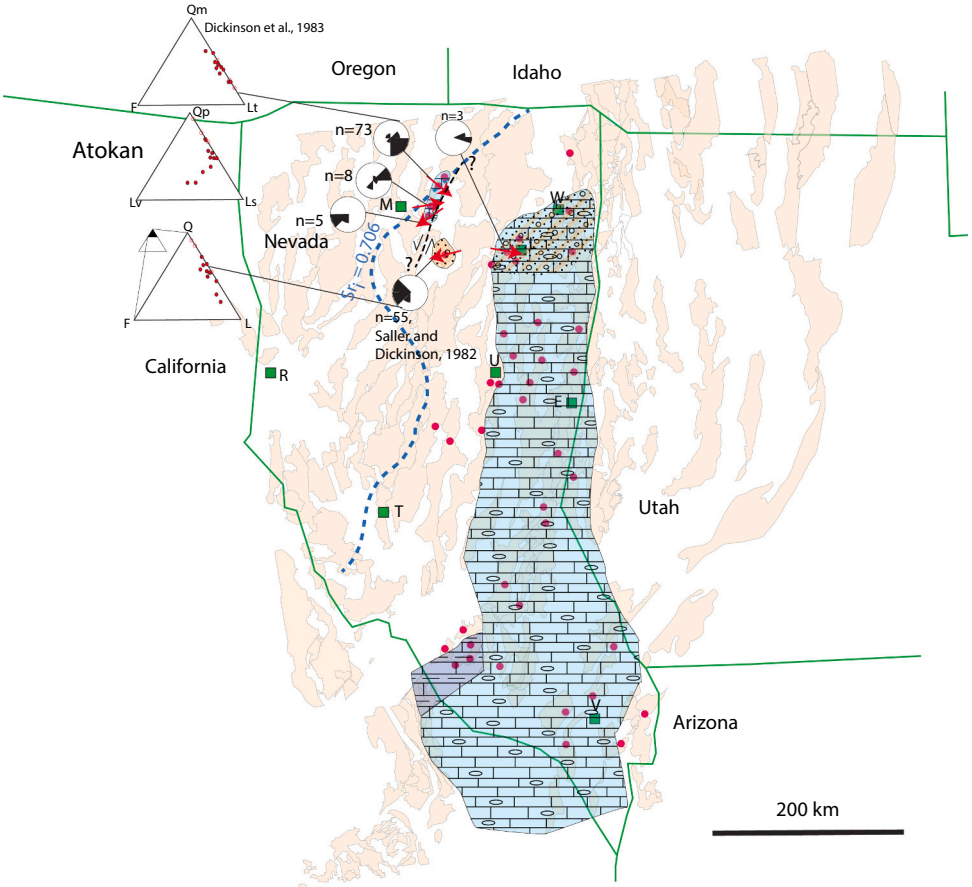


**Fig. 12.** Paleogeographic map for Atokan time on the late Paleozoic reconstructed base map (Fig. 5). Maps show estimated minimum extents of depositional belts (patterned). Paleocurrent data from Saller and Dickinson (1982) and unpublished data from Trexler Jr. Compositional data from Dickinson et al. (1983). E, Ely; L, Elko; M, Winnemucca; R, Reno; T, Tonopah; U, Eureka; V, Las Vegas; W, Wells.

allochthonous sections (Fig. 2, # 32–33). The chert litharenite beds in the autochthonous section show that the turbidite trough was still active in late Chesterian time, but we have no direct record of the late Chesterian history along the basin axis at the southern end of the turbidite basin (Trexler Jr. and Cashman, 1997).

### 4.6. Atokan

In Morrowan to Atokan time a broad, shallow carbonate shelf formed across eastern and southern Nevada atop the C3 unconformity surface. The sea-level drop during latest Mississippian time (e.g., Ross and Ross, 1987; Lane et al., 1999) resulted in subaerial exposure of most of the study area and formation of the C3 unconformity. Notably, in contrast to the other unconformities (Fig. 12), this unconformity is not associated with sub-unconformity structures or tilting. As sea level rose in the Early Pennsylvanian, the Mississippian clastic Antler Successor Basin was replaced by the broad, shallow-water Ely-Bird Spring Carbonate Shelf (e.g., Stevens and Stone, 2007; Sturmer, 2012). In contrast to the northeast-southwest to north-south oriented facies belts throughout the Mississippian, the carbonate shelf covers most of the study area from the latitude of Wells, NV to southeastern California (Stevens and Stone, 2007) and from central Nevada into western Utah (Fig. 12).

The carbonate shelf is characterized by repeated, coarsening-upward cycles (e.g., Dott Jr., 1955, 1958; Stevens and Stone, 2007; Bishop et al., 2010; Martin et al., 2012; Sturmer et al., 2021). The cycle bases are dominated by mudstone and wackestone, grading upward into packstone, grainstone, and occasionally siliciclastic sandstone or conglomerate beds (e.g., Dott Jr., 1955; Stevens and Stone, 2007; Bishop et al., 2010; Martin et al., 2012; Sturmer, 2012). Finer-grained cycle bases are commonly poorly exposed. Sections within the basin contain between 25 and 40 of these cycles (e.g., Sturmer, 2012; Sturmer et al., 2021). The cycles range in thickness from a few meters to a few tens of meters (e.g., Lane et al., 1999; Saltzman, 2003; Tierney, 2005; Stevens and Stone, 2007; Sturmer, 2012). The cycles are interpreted as recording cyclic sea level change during the Late Paleozoic Ice Age (e.g., Dott Jr., 1958; Lane et al., 1999; Saltzman, 2003; Scott and Elrick, 2004; Tierney, 2005; Bishop et al., 2010; Martin et al., 2012; Sturmer, 2012). Depositional environments range from outer ramp (fine-grained cycle bases) to nearshore/fluvio-deltaic (coarse-grained cycle tops) (Stevens and Stone, 2007; Bishop et al., 2010; Martin et al., 2012). The cycles are therefore interpreted as recording the transition from maximum flooding near cycle bases to sea-level lowstands at cycle tops.

In Atokan time, conglomerate beds periodically prograded from the west across northern Nevada during times of sea-level lowstand (e.g., Dott Jr., 1955; Sweet, 2003; Sturmer, 2012). Sandstone and conglomerate beds are present in Atokan strata at the Central Pequop Mountains, Carlin Canyon, and Grindstone Mountain sections (Fig. 2, # 8, 10, 11; Dott Jr., 1955; Sweet, 2003; Sturmer, 2012; Sturmer et al., 2021). Conglomerate beds cap lithological cycles, occurring above packstone/grindstone beds and below mudstone-rich cycle bases (Dott Jr., 1955; Sweet, 2003; Sturmer, 2012; Sturmer et al., 2021). Conglomerates generally contain pebble-sized chert and quartzite clasts, likely sourced either from the RMA or from uplifted Mississippian conglomeratic units. Near Elko (Fig. 2, #10, 11) conglomerate abundance increases to ~50% toward the top of the section with beds up to 60 m thick (Dott Jr., 1955). These beds likely represent the distal edges of prograding fluvio-deltaic systems during sea-level lowstands. Conglomerate and sandstone beds have been documented in the northern part of the basin only (Fig. 12).

The broad carbonate shelf did not extend to the northwesternmost part of the study area (Fig. 2, #1–5). Deposition in this area didn't resume until Morrowan time following moderate to deep erosion during C2 and the Late Mississippian (Fig. 12). Initial deposition was pebble to boulder quartzite conglomerate and interbedded channel sandstone at Edna Mountain (Villa, 2007; Cashman et al., 2011). These deposits are interpreted to record an alluvial fan to fluvio-deltaic environment (Saller and Dickinson, 1982; Villa, 2007; Cashman et al., 2011). Late in Morrowan time, the conglomerates from the Dry Hills south to Edna Mountain gave way to a shallow marine, mixed clastic-carbonate system which persisted into middle Atokan time (Fig. 2, #1–4; Ferguson et al., 1951, 1952; Villa, 2007; Cashman et al., 2011). Rocks of this age include interbedded sandy to silty wackestone, packstone, and grainstone interbedded with calcareous sandstone and conglomerate. The conglomerate is poorly sorted and contains angular quartzite and chert pebbles (Cashman et al., 2011). Clastic units show paleocurrents predominantly to the southeast with subordinate flow to the east-northeast and west-southwest (Fig. 12; Saller and Dickinson, 1982). Farther east, alluvial fan conglomerate grading upward into fluvio-deltaic conglomerate and sandstone was deposited at Battle Mountain (Fig. 2, #5; Saller and Dickinson, 1982). Paleocurrents at Battle Mountain were dominantly to the west and southwest (Fig. 12; Saller and Dickinson, 1982).

The deepest water Atokan carbonate deposits are preserved in the southwestern part of the study area at Syncline Ridge on the Nevada National Security Site (Fig. 2, #34). The strata are dominantly poorly-exposed thin-bedded silty mudstone with cyclic 0.5 to 3 m thick grainstone beds. Farther up section, the grainstone beds are replaced with periodic thin debrite and carbonate turbidite beds. Fossils are rare, with locally abundant gastropods (Titus and Manger, 1992; Sturmer, 2012; Sturmer et al., 2021). The combination of mudstone with event beds and turbidites is consistent with deposition in an outer shelf to upper slope setting as part of a distally-steepened ramp (Yose and Heller, 1989; Miller and Heller, 1994; Stevens et al., 2001; Sturmer, 2012). We interpret these strata to represent a connection between the Bird Spring Shelf to the east and the Keeler Basin to the west (Yose and Heller, 1989; Miller and Heller, 1994; Stevens et al., 2001; Stevens and Stone, 2007).

### 4.7. C5 and C6 unconformity surfaces

The C5 and C6 unconformities document significant tectonic shortening, uplift, and erosion in northern and central Nevada during a relatively short period in Middle Pennsylvanian time (Figs. 13 and 14). Though they are demonstrably separate surfaces, both are not always present because C6 cuts down-section and removes C5 across much of the study area. Both unconformities are present in a few localities in eastern Nevada, where they are separated by strata of the Hogan Basin. Both unconformities also appear to be preserved at Edna Mountain (Fig. 2, #4), in the translated Edna Block at the northwestern edge of the study area. Structures below C5 are northwest-vergent overturned folds and northwest-directed thrust faults. In the western part of the study area where C5 has been removed by erosion, the structures below C6 are also northwest-vergent, suggesting that these structures, too, formed during pre-C5 shortening. At Edna Mountain, (Fig. 2, #4), sub-C5 structures are truncated by a low-angle normal fault and rotated counter-clockwise around a vertical axis. Deposition continued in southern Nevada but documents a shift to shallower and locally more restricted depositional environments.

The C5 and C6 unconformities formed across the northern three-quarters of the study area during the early Desmoinesian and late Desmoinesian to Missourian times, respectively. Both the C5 and C6 unconformities are angular. C5 cut down to the east whereas C6 cut deeply down to the west, removing older unconformities (e.g., Trexler Jr. et al., 2004; Sturmer et al., 2018). For example, at Carlin Canyon (Fig. 2, # 10), C6 cut down to the Upper Mississippian, removing several hundred meters of Lower Pennsylvanian strata present just a few km to the east (Trexler Jr. et al., 2004). The result is that C6 completely removes C5 across much of the study area. The main exception is the narrow area where middle Desmoinesian sediments of the Hogan Formation are preserved (Fig. 14). Youngest strata preserved below C5 are upper Atokan in age, but may be as young as lower Desmoinesian at Illipah Reservoir and near Elko (e.g., Dott 1955; Sturmer, 2012; Sturmer et al., 2021). Strata preserved between C5 and C6 are middle to upper Desmoinesian in age (e.g., Robinson Jr., 1961; Sweet, 2003; Pérez-Huerta, 2004; Cashman et al., 2011). Oldest strata deposited atop C6 are middle

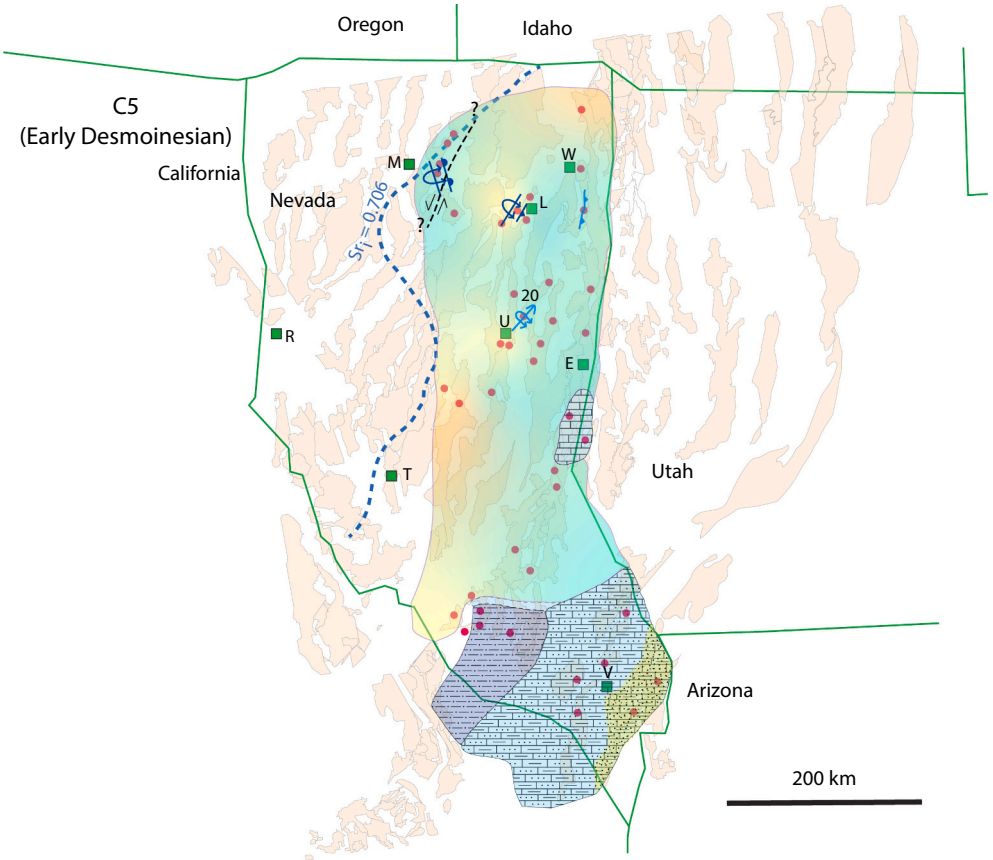


**Fig. 13.** Paleogeographic map for the C5 unconformity (early Desmoinesian) on the late Paleozoic reconstructed base map (Fig. 5). Maps show estimated minimum extents of depositional belts (patterned). Structure symbols show general orientation and style of deformation preserved in strata below the unconformity (Sweet, 2003; Trexler Jr. et al., 2004; Cashman et al., 2011; Whitmore et al., 2021). Color ramp represents depth of erosion inferred from age of unit below the unconformity (see Fig. 6). Light blue represents area of inferred shallow-water deposition between deep marine deposition and subaerial exposure. E, Ely; L, Elko; M, Winnemucca; R, Reno; T, Tonopah; U, Eureka; V, Las Vegas; W, Wells. (For interpretation of the references to colour in this figure legend, the reader is referred to the web version of this article.)

Missourian (e.g., Sweet, 2003; Trexler Jr. et al., 2004).

Structures below the C5 unconformity include distinctive NW-vergent folds and top-to-the-NW thrust faults. They record NW-SE shortening, and are preserved in the Pequop Mountains and at Buck Mountain (Fig. 2, #8, 16) (Sweet, 2003; Trexler Jr. et al., 2004; Whitmore et al., 2021). Structures of this age are not present at the Illipah Reservoir section just SE of Buck Mountain (Fig. 2, # 19), thus constraining the southeastern extent of the deformation (Sturmer, 2012; Whitmore et al., 2021). The C6 unconformity cuts down-section west of these localities, removing the C5 unconformity and the overlying Hogan Formation. Although it's impossible to determine the age of the sub-C6 structures where C5 is absent (e.g., Carlin Canyon (Fig. 2, #10)), the distinctive northwest vergence of the dominant folds argues for them being cogenetic with the sub-C5 structures. Both the C5 and C6 unconformities also appear to be present at Edna Mountain, in the translated Edna Block at the northwestern edge of the study area (Fig. 2, # 4).

Structures at Edna Mountain (Fig. 2, #4) verge WSW, differing in orientation but not style from sub-C5 structures observed farther east and southeast (Villa, 2007; Cashman et al., 2011). The WSW-vergent folds were followed by top-to-the-northeast motion on the Iron Point Fault, a low-angle normal fault. Although originally mapped as the Iron Point Thrust Fault (Erickson and Marsh, 1974a, 1974b, 1974c), this fault places younger rocks over older, and associated small-scale structures include brecciation, veining and iron staining, which are typical of extensional faults. It was reinterpreted as a tectonic unroofing structure that formed in response to extreme crustal thickening (Villa, 2007; Cashman et al., 2011). The distinctive style and vergence of the folds is similar to sub-C5 folds elsewhere, but fold axes are rotated ~60° counter-clockwise. This rotation is consistent with drag along the NW-striking fault in the eastern edge of Edna Mountain, indicating a sinistral sense of offset (Key and Cashman, 2021).

Sedimentation was continuous through Desmoinesian and into Missourian time in much of southern Nevada, with a shift to shallower water and locally restricted deposition (e.g., Bishop et al., 2010; Martin et al., 2012). Rock types vary across the shelf, including mudstone, heterozoan and photozoan packstone, grainstone, dolomudstone, and cross-bedded quartz siltstone (Martin et al., 2012). Depositional environments range from outer platform/upper slope to restricted platform interior and beach, generally shallowing to the south and southeast (e.g., Rice, 1990; Martin et al., 2012). Farther west, deposition of shale punctuated by thin turbidite beds continued on the Tippipah Slope (NNSS) during C5 time (Sturmer, 2012). Depositional patterns did change during C6 time, with coarser-grained turbidites on the Tippipah Slope and exposure with development of an unconformity in the far southeastern part of the study area (e.g., Rice, 1990; Sturmer et al., 2021).

### 4.8. *Middle Desmoinesian*

The middle Desmoinesian rock record is incomplete, and accordingly somewhat ambiguous, because of erosion along the closely spaced C5 (early Desmoinesian) and C6 (late Desmoinesian-Missourian) unconformities (Fig. 14). The absence of mid-Desmoinesian rocks in northern and central Nevada may reflect either non-deposition or erosional truncation by the C6 unconformity. Preserved middle Desmoinesian rocks of the Hogan Basin record a relatively deep basin exposed in a narrow belt of mountain ranges between Wells and Ely. Although carbonate deposition continued in west-central Utah, these formations were relatively shallow and punctuated by disconformities (Ritter and Robinson, 2009). Deposition in southern Nevada was dominated by a carbonate shelf, transitioning into aeolian deposits to the east and slope shale and turbidites to the west (Fig. 14).

The Hogan Basin of northeastern Nevada represents a significant deepening of the depositional environment (Sweet, 2003; Schiappa

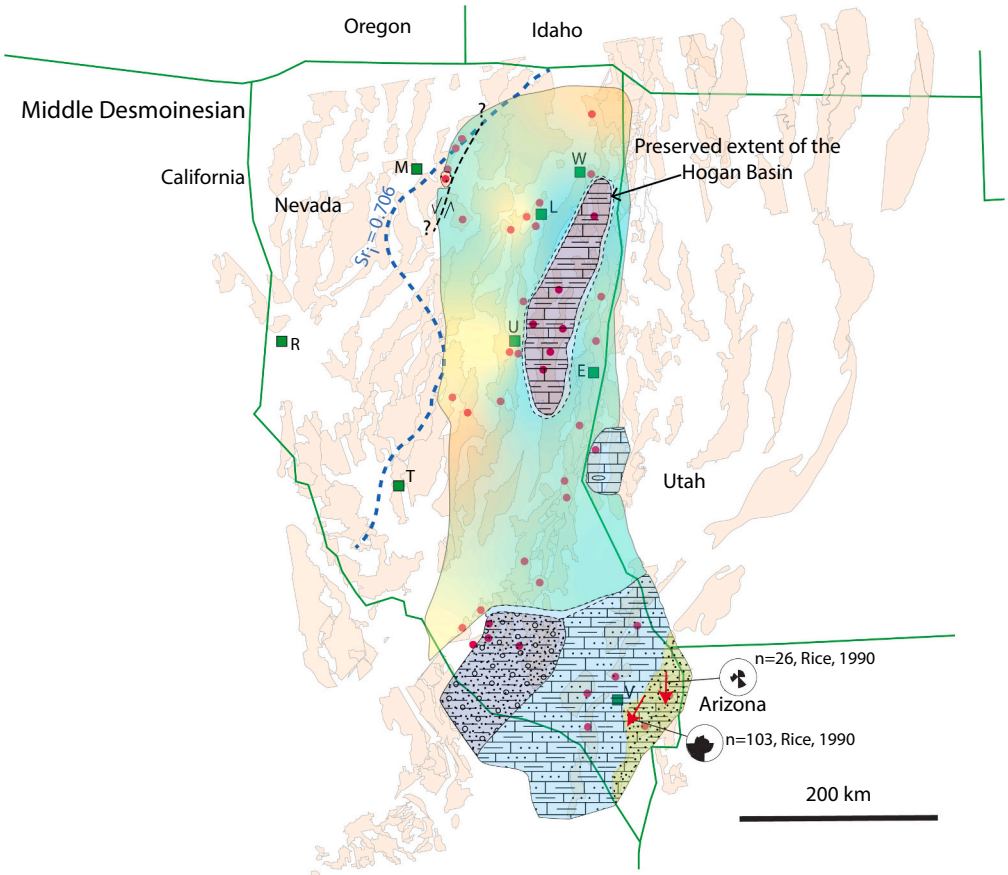


**Fig. 14.** Paleogeographic map for middle Desmoinesian time on the late Paleozoic reconstructed base map (Fig. 5). Maps show estimated minimum extents of depositional belts (patterned). Color ramp represents depth of erosion inferred from age of unit below the unconformity (see Fig. 6). Light blue represents area of inferred shallow-water deposition between deep marine deposition and subaerial exposure. Paleocurrent data from Rice (1990). E, Ely; L, Elko; M, Winnemucca; R, Reno; T, Tonopah; U, Eureka; V, Las Vegas; W, Wells. (For interpretation of the references to colour in this figure legend, the reader is referred to the web version of this article.)

et al., 2017; Sturmer et al., 2018). Strata within the Hogan Basin are mostly calcareous siltstone, mudstone, and wackestone (Robinson Jr., 1961; Mollazal, 1961; Payne and Schiappa, 2000; Sweet, 2003; Pérez-Huerta, 2004; Whitmore, 2011). These deposits have been interpreted as relatively deep marine, based on textural and faunal evidence (Sweet, 2003; Schiappa et al., 2017). Northern exposures of basin strata at the central Pequop Mountains (Fig. 2, #8), contain a few 0.5–2.5 m thick grainstone beds with sharp basal contacts, interpreted as turbidite deposits (Sweet, 2003). Farther south at Buck Mountain (Fig. 2, #16), Hogan Formation rocks are predominantly flaggy-weathering sandy siltstone, with local thinly-bedded petroliferous carbonate mudstone. The preserved thickness is variable and is locally less than 10 m; the original thickness is unknown (Whitmore, 2011). The ammonoid *Somoholites* n. sp. has been identified in the cores of concretions in the silty mudstone at Buck Mountain (Schattauer and Schiappa, 2010). These observations are consistent with Hogan Formation rocks being deposited in a deep basin with good circulation (Schiappa et al., 2017). Poor exposure combined with limited preservation, most notably due to erosion along the C6 surface, precludes a more detailed tectonic interpretation of the Hogan Basin at present.

The carbonate basin in western Utah was dominated by mid- to upper ramp wackestone and packstone (St. Aubin-Hietpas, 1983; Ritter and Robinson, 2009). Strata are m-scale shallowing-upward strata with muddy heterozoan wackestone grading upward into photozoan packstone (Ritter and Robinson, 2009). These units are punctuated by biostromes of *Komia, Palaeoaplysina,* and *Syringopora*, indicating openly circulating marine water (Ritter and Robinson, 2009). These middle Desmoinesian sediments are disconformably overlain by a thin upper Desmoinesian dolomudstone parasequence representing more restricted circulation patterns (Ritter and Robinson, 2009).

Middle Desmoinesian strata are missing in the northwestern part of the study area, except for a distinctive conglomerate unit at Edna Mountain (Fig. 2, #4). It was deposited locally within depressions on a karsted surface (Cashman et al., 2011). Clasts, dominantly angular silty limestone and red or green phyllite, were derived from the underlying Highway Limestone and Preble Formation, respectively (Villa, 2007; Cashman et al., 2011). The rare occurrences of clast imbrication are consistent with north-directed paleocurrents (Cashman et al., 2011).

Deposition on the Bird Spring Shelf in southern Nevada continued through Desmoinesian time, with shallower facies, an increase in aeolian clastic input, and a shift to more restricted conditions (Welsh, 1959; Gamache, 1986; Sur et al., 2010; Martin et al., 2012; Sturmer et al., 2018). Facies are dominated by heterozoan and photozoan packstone and grainstone, calcareous siltstone, peloidal grainstone, boundstone, and dolomudstone (Martin et al., 2012). Many of the carbonate units include fine-grained sand interpreted as having an aeolian origin (Sur et al., 2010). Depositional environments are interpreted as low- and high-energy inner platform and restricted platform, with increasing abundance of the restricted facies upsection (Martin et al., 2012). To the east, Bird Spring Basin deposits transition into aeolian carbonate units exposed in southeastern Nevada and northwestern Arizona (Rice, 1990). This area is dominated by marine limestone, with increasing abundance of carbonate aeolian deposits. Farther south and east, the strata become more siliceous, and abundance of aeolian and fluvial deposits increases, with no marine limestones present in the Grand Canyon area (e.g., McKee, 1982; Blakey, 1990; Rice, 1990; Gehrels et al., 2011). Paleocurrent directions are consistently toward the south to south-southwest in the aeolian units (Rice, 1990).

Deepwater deposition continued at Syncline Ridge (Fig. 2, #34) with increased conglomeratic turbidite beds beginning in middle Desmoinesian time. Conglomerates are dominantly clast-supported (locally matrix-supported), containing contorted rip-up clasts and angular to rounded limestone and chert pebbles. The conglomerate units are commonly cross-bedded and associated with soft-sediment deformation

features including slump folds. Packstone and grainstone units are interbedded with the conglomerate, including local phylloid algal and crinoid bioherms (unpublished data, Trexler Jr. et al., 1996). Overall, these units are interpreted as a combination of turbidites and debris flows, still perhaps in an outer shelf to upper slope depositional environment (e.g., Miller and Heller, 1994). Farther west, turbidites, megabreccias, and debris flows began to be deposited within the deep-water Keeler Basin (Yose and Heller, 1989; Miller and Heller, 1994). The changes in deposition style have been interpreted to represent a change from a distally-steepened ramp in Early Pennsylvanian time to a rimmed shelf beginning in Desmoinesian time (Yose and Heller, 1989; Miller and Heller, 1994; Stevens et al., 2001; Bishop et al., 2010). The Syncline Ridge area therefore represents the shallower reaches of the connection between the Bird Spring Shelf and the Keeler Basin (Yose and Heller, 1989; Miller and Heller, 1994; Sturmer, 2012). Elsewhere at the NNSS and at Bare Mountain, there are no known Paleozoic deposits younger than late Chesterian in the allochthonous thrust sheets (e.g., Cole and Cashman, 1999).

## 5. Discussion and geologic history

Of the six Mississippian and Pennsylvanian unconformities recognized by Trexler and Snyder (C1 – C6, in Trexler Jr. et al., 2003, 2004) (Fig. 1), it is now clear that only three are tectonically significant. The C3 and the C4 unconformities are not associated with angular truncations, and both were formed during global sea-level lowstands (Fig. 1). They are interpreted here to be non-tectonic in origin. In contrast, widespread angular truncations and sub-unconformity structures are associated with the late Middle Mississippian C2 and Middle Pennsylvanian C5 and C6 unconformities. These are clearly tectonic.

The latest Devonian unconformity (C1 of Trexler Jr. et al., 2003, 2004) marks a sea-level lowstand; it has also long been defined as a significant tectonic marker. Evidence for subaerial exposure and erosion is found locally on this surface; for example, at Shoshone Mountain and Mine Mountain on the NNSS (e.g., Fig. 2, #35), fine-grained siliciclastic rocks overlie the karst surface on the Upper Devonian carbonates (Trexler Jr. et al., 1996; French et al., 2020). However, angular truncations are absent at these locations, so this unconformity does not record tectonism. It does record the initiation of "western facies" siliciclastic sedimentation on the Upper Devonian continental margin carbonates. For this reason, the contact has long been interpreted as the initiation of Antler Foreland Basin deposition, and therefore used to date the Antler Orogeny (Roberts et al., 1958; Nilsen and Stewart, 1980). However, the lack of an angular unconformity and of coarse-grained synorogenic sediments indicates that C1 should *not* be used as a marker of the Antler Orogeny.

There was a significant time lag between initial siliciclastic deposition in the Antler Foreland Basin and the arrival of coarse-grained synorogenic deposits in the study area (Figs. 7-8). Although the initial fine-grained clastic sediments are uppermost Devonian, coarse-grained synorogenic sediment did not arrive in the foreland basin in Nevada until Osagean time (Trexler Jr. and Cashman, 1997; Trexler Jr. et al., 2003, and references therein). This is a lag of about 10 Myr. The coarse-grained sediment originated to the northwest of the Laurentian margin and flowed south as turbidites along the axis of the foreland basin, parallel to the continental margin (Fig. 8). The absence of contemporaneous exposures to the northwest precludes a better understanding of the tectonic setting at the sediment source. An Osagean unconformity in turbidites of the Copper Basin Group in Idaho (Link et al., 1996) records tectonism farther north at this time, but is most likely not a direct sediment source for the foreland basin in Nevada.

Late Middle Mississippian tectonism was widespread and substantial. It formed the earliest documented structures in the Antler Foreland Basin of Nevada. The tectonic uplift was greatest to the northwest, and the resulting erosion surface (C2) covered the entire northern half of the study area (Fig. 9). The C2 contact can be identified in the subsurface, and has been mapped across Nevada (French et al., 2020). Where most tightly constrained, the tectonism occurred between late Osagean and earliest Chesterian time (Trexler Jr. et al., 2003). Sediment had been accumulating in the foreland basin for at least 20 and possibly as many as 30 Myr prior to this deformation (Trexler Jr. et al., 2003). In the translated Edna Block (Fig. 2, #1–4), Morrowan and Atokan rocks directly overlie the unconformity, indicating that this area remained high throughout Chesterian time. Concurrently, sedimentation had resumed in the Antler Successor Basin farther south and east. Geometric and kinematic data unequivocally recording late Middle Mississippian tectonism are limited to structures in clastic rocks of the Antler Foreland Basin that are overlain unconformably along C2 by undeformed rocks of the Antler Successor Basin (Fig. 9) (e.g., Trexler Jr. et al., 2003, and references therein). A few localities in north-central Nevada record east- or east-southeast-directed thrust faults (e.g., Tosdal unpublished mapping in Trexler Jr. et al., 2003) (Fig. 2, # 12), and angular unconformities record eastward dips (Fig. 2, #10, 12). However, in the Snake Mountains to the northeast (Fig. 2, # 6), folds and thrust imbrications in Antler Foreland Basin rocks record significant southeast-directed shortening immediately below the RMT (McFarlane, 1997, 2001). This geographic distribution of late Middle Mississippian structures, supported by an eastward step in the $Sr_i$ 0.706 line in northeastern Nevada (Fig. 4), indicates that there was an eastward step in the continental margin at this latitude (e.g., McFarlane, 2001). At present, it is not clear whether the different orientations of sub-C2 structures represent original shortening directions, or a partial record of strain partitioning across the Laurentian margin. However, the orientation of the C2 boundary (Fig. 9) supports a locally NE-trending continental margin with NW-SE shortening across it in late Middle Mississippian time.

Strata of the Antler Successor Basin overlie the angular C2 unconformity and record a fluvial-deltaic system grading up into a broad carbonate platform. The fluvio-deltaic system built south and east from the tectonic highland (Figs. 10-11). Although this paleogeographic setting contrasts dramatically with the turbidite-dominated foreland basin below the C2 unconformity, early stratigraphic terminology in Nevada did not distinguish between rocks deposited in these two basins. The terminology therefore delayed recognition of the C2 unconformity, and of the late Middle Mississippian tectonism that produced it. In latest Mississippian time clastic material periodically washed in from the east, locally interfingering with the fluvio-deltaic and deeper sediments sourced from the west and northwest (Fig. 11). Following the end-Mississippian sea-level lowstand, most of the study area was covered by a shallow-marine carbonate shelf (Fig. 12). Basin depositional patterns were driven by glacioeustacy. By Atokan time, rapid subsidence began in the northwestern part of the basin (e.g. Sturmer, 2012; Sturmer et al., 2012, 2018; 2021). Periodic progradation of clastic deposits during sea-level lowstands also began in Atokan time in the northern part of the basin, generally increasing in frequency upsection.

Vigorous tectonic activity resumed in Middle Pennsylvanian time, producing structures across the width of the study area, followed by subaerial exposure that resulted in extensive erosion surfaces. The two-stage event produced two geographically adjacent tectonic highlands, which eroded to form the C5 (late Atokan – early Desmoinesian) and C6 (late Desmoinesian – middle Missourian) unconformities (Fig. 13). Rocks of the Desmoinesian Hogan Formation were deposited between the C5 and C6 unconformities and record relatively deep-water conditions during this time (Robinson Jr., 1961; Mollazal, 1961; Payne and Schiappa, 2000; Sweet, 2003; Pérez-Huerta, 2004). On-going work on the internal stratigraphy of the Hogan Formation will shed light on the original extent, shape and tectonic setting of the Hogan Basin. Structures below the Hogan Formation include northwest-vergent overturned folds and northwest-directed thrust faults; they pre-date the C5 unconformity (e.g., Trexler Jr. et al., 2004; Cashman et al., 2011, 2016, 2020). Because the C6 unconformity cut down-section toward the west and eroded through both the C5 unconformity and the Hogan Formation, the original extents of both are unknown.

Each of the Middle Pennsylvanian tectonic events is associated with subsidence of a relatively deep basin. The northwestern edge of the Pennsylvanian carbonate shelf (Fig. 2, # 11; Fig. 12) subsided rapidly in earliest Atokan time. This subsidence preceded formation of the C5 unconformity. The subsidence curve is consistent with flexural subsidence due to structural loading (Sturmer, 2012; Fig. 16 in Sturmer et al., 2021); the original shape and extent of this deep basin are unknown. The deep Hogan Basin (Fig. 14) preceded the formation of the C6 unconformity; it, too, may have formed in response to structural loading. Alternatively, it could be a graben, strike-slip or composite basin analogous to the Kinderhookian basins in Idaho (e.g., Wilson et al., 1994; Link et al., 1996). Further work is underway to determine the initial shape and extent of the Hogan Basin.

The shortening direction was NW-SE, notably not W-E, in this part of Laurentia during Mississippian-Pennsylvanian time. Sedimentological evidence documents a sediment source to the northwest and a regional topographic gradient downward toward the southeast: synorogenic coarse-grained sediment entered the basins from the NW and was transported S parallel to the margin in Mississippian time (Figs. 8, 10, 11). At times of subaerial exposure in northern Nevada, submarine deposition continued in southern Nevada, and the coastline was oriented SW-NE (Figs. 9, 13, 14). Structures formed in the Middle Mississippian event record either W-E or NW-SE shortening and those formed in Middle Pennsylvanian time record NW-SE shortening: fold axes trend NE (e.g., Trexler Jr. et al., 2004). Thrust faults are generally SE- or NW-directed, (e.g., McFarlane, 1997; Trexler Jr. et al., 2004; Key and Cashman, 2021; Whitmore et al., 2021). The fastest localized subsidence of the Early to Middle Pennsylvanian Ely-Bird Spring Basin was in the NW (Sturmer, 2012; Sturmer et al., 2021). This NW-SE shortening is consistent with a sinistral-convergent margin along the western edge of Laurentia during late Paleozoic time (Lawton et al., 2017). It contrasts with the direction predicted by many other tectonic models for southwestern Laurentia in the late Paleozoic (e.g., Burchfiel and Davis, 1972, 1975; Nilsen and Stewart, 1980; Speed and Sleep, 1982; Burchfiel et al., 1992; Dickinson, 2000; Leary et al., 2017).

The deep erosion of the Edna Block (Fig. 2, #1–4) requires three phases of anomalous tectonic uplift and significant lateral offset along a margin-parallel fault. Edna Mountain itself (Fig. 2, #4), records tectonic uplift and subaerial exposure associated with the C2, C5 *and* C6 unconformities. First, Upper Morrowan rocks directly overlie Cambrian rocks on the C2 unconformity, recording erosion of the entire post-Cambrian section. This documents dramatic uplift and prolonged subaerial exposure of the Edna Block associated with Late Mississippian tectonism. Second, an angular, locally derived conglomerate fills a karsted C5 surface on folded and faulted Atokan limestone. This surface post-dates west-vergent folding and tectonic denudation by the Iron Point low-angle normal fault, and records significant crustal thickening and tectonic uplift in middle Desmoinesian time. Third, this conglomerate is itself unconformably overlain by Upper Pennsylvanian limestone atop the C6 unconformity, recording another period of subaerial exposure. The eastern boundary of the Edna Block is a high-angle fault, or faults. The easternmost of these is in eastern Edna Mountain (Fig. 2, #4), where a N-striking fault separates the Pennsylvanian-on-Cambrian rocks from a thick autochthonous Ordovician section (Key, 2015; Key and Cashman, 2021). Tectonic rotation of the pre-C5 folds in the Edna Block suggests sinistral-oblique motion on the fault. At the next locality to the east, Battle Mountain (Fig. 2, #5), Pennsylvanian rocks are deposited on the RMA (Ferguson et al., 1952; Roberts et al., 1958; Roberts, 1964; Saller and Dickinson, 1982), hinting that additional fault strand(s) may bound the Edna Block on the east. The distinctive nature of the Edna Block (Fig. 2, #1–4) was previously noted, based on the unique presence of pre-Middle Pennsylvanian metamorphism and polyphase deformation (Jones Crafford, 2008).

Several of the above observations are consistent with a sinistral component of offset along western margin of Laurentia as proposed by previous workers. A southward-propagating sinistral-oblique convergent margin documented in the Canadian Arctic, Yukon, and northwestern Canada reached the area of present-day British Columbia by Devonian time (Colpron and Nelson, 2009). Late Middle Mississippian tectonism in Nevada is consistent with this pattern. Detrital zircons from the RMA and from the Harmony Formation, its structurally highest unit, match sources in northwestern Canada; they are thought to have been transported structurally to their present location (Linde et al., 2016, 2017). SE-directed imbrication of the RMA with foreland basin rocks as far east as the Snake Mountains (McFarlane, 1997, 2001) can be explained by oblique convergence, where translated rocks encounter an eastward step in the Laurentian margin. Direct evidence of translation along the margin is evident in the unusual uplift and extended erosion of the Edna Block (Fig. 2, #1–4). It was translated to its present position; counter-clockwise rotation of the Middle Pennsylvanian fold set indicates that the translation was sinistral. Anomalously rapid subsidence of the northwestern edge of the Pennsylvanian carbonate platform (e.g., Sturmer, 2012; Sturmer et al., 2018; 2021) suggests that area records the initial Middle Pennsylvanian tectonism. Lastly, both pre-C2 and pre-C5 structures record NW-SE shortening; this is consistent with sinistral oblique convergence, but not with previous models of eastward obduction.

## 6. Conclusions

Compilation of stratigraphic, sedimentological, and structural data on palinspastically restored maps reveals the Mississippian – Middle Pennsylvanian paleogeography and evolution of southwestern Laurentia in unprecedented detail. These maps record two major periods of tectonism, in late Middle Mississippian and Middle Pennsylvanian time. Syn-orogenic sediments came from the northwest. Folds and thrust faults record NW-SE shortening. Subaerial erosion produced widespread unconformities in northern and central Nevada at both times, while deposition continued in southern Nevada. Notably, there are no structures formed in Late Devonian-Early Mississippian time, the age previously cited for the Antler Orogeny. A transported crustal block, herein named the Edna Block, records a similar tectonic history, but with tighter folds and deeper, more prolonged erosion. Both suggest more extreme shortening and uplift of the Edna Block than of the autochthonous Laurentian margin. The Edna Block was most likely emplaced late in the Middle Pennsylvanian tectonic event; it was in its present position at the northwest edge of the study area before the Permo-Triassic Sonoma Orogeny.

This detailed re-examination of the rocks in Nevada that inspired the “Antler Orogeny” demands a dramatic revision of that paradigm. The rocks record tectonism at multiple times, rather than just one. Late Paleozoic tectonism in Nevada did not start until late Middle Mississippian time, rather than latest Devonian. Shortening was northwest-southeast, oblique to the Laurentian margin, rather than perpendicular to it. These observations are consistent with evolving sinistral-oblique convergence along the Laurentian margin. Future usage of the term “Antler Orogeny” must be altered accordingly.

## Declaration of Competing Interest

The authors declare that they have no known competing financial interests or personal relationships that could have appeared to influence the work reported in this paper.

## Acknowledgments

Although this research did not receive any specific grant from funding agencies in the public, commercial, or not-for-profit sectors, it is the culmination of decades of work, much of it funded by grants from NSF and from the Nevada Nuclear Waste Projects Office to Pat Cashman, Jim Trexler and their colleagues. This work would not have been possible without the dedicated effort and contributions of James H.

Trexler, Jr. Jim greatly advanced our understanding of late Paleozoic tectonics in Nevada, and we miss him. The maps presented here incorporate the work of many graduate students from the University of Nevada, Reno, Boise State University, the University of Nevada, Las Vegas, and Slippery Rock State University who were supervised by the authors and their colleagues. We also thank Walt Snyder, Vladimir Davydov, Tamra Schiappa, Jim Cole, Wanda Taylor, Don French, Jerry Walker, Norm Silberling, and Scott Ritter for their contributions to our understanding of late Paleozoic tectonics and sedimentation in Nevada. Also, thanks to Nadine McQuarrie for providing her 36 Ma reconstructed maps that were restored for this study. This manuscript was improved by reviews from Tim Lawton and an anonymous reviewer and editorial handling by Dustin Sweet and Tom Algeo.

## Appendix A. Supplementary data

Supplementary data to this article can be found online at https://doi.org/10.1016/j.palaeo.2021.110666.

## References

Axen, G.J., 1984. Thrusts in the eastern Spring Mountains, Nevada: geometry and mechanical implications. GSA Bull. 95, 1202–1207.
Best, M.G., Hintze, L.F., Deino, A.L., Maughan, L.L., 1998. Geologic map of the Fairview Range and Grassy Mountain, Lincoln County, Nevada. In: Nevada Bureau of Mines and Geology Map, 114 (Scale 1:24,000).
Bishop, J.W., Montañez, I.P., Gulbranson, E.L., Brenckle, P.L., 2009. The onset of mid-Carboniferous glacio-eustasy: sedimentology and diagenetic constraints, Arrow Canyon, Nevada. Palaeogeogr. Palaeoclimatol. Palaeoecol. 276, 217–243.
Bishop, J.W., Montañez, I.P., Osleger, D.A., 2010. Dynamic Carboniferous climate change, Arrow Canyon, Nevada. Geosphere 6, 1–34.
Blakey, R.C., 1990. Stratigraphy and geologic history of Pennsylvanian and Permian rocks, Mogollon Rim region, central Arizona and vicinity. GSA Bull. 102, 1189–1217.
Brenckle, P.L., Baesemann, J.F., Lane, H.R., West, R.R., Webster, G.D., Langenheim, R.L., Brand, U., Richards, B.C., 1997. Arrow Canyon, the mid-Carboniferous boundary stratotype. In: Brenckle, P.L., Page, W.R. (Eds.), Paleoforams '97 Guidebook Post-Conference Field Trip to the Arrow Canyon Range, Southern Nevada, USA: Cushman Foundation for Foraminiferal Research Supplement to Special Publication Number, 36, pp. 13–32.
Brew, D.A., Gordon Jr., M., 1971. Mississippian stratigraphy of the Diamond Peak area, Eureka County, Nevada. In: USGS Professional Paper, 661, 84 p.
Burchfiel, B.C., Davis, G.A., 1972. Structural framework and evolution of the southern part of the cordilleran orogeny, western United States. Am. J. Sci. 272, 97–118.
Burchfiel, B.C., Davis, G.A., 1975. Nature and controls of Cordilleran orogenesis, western United States: extensions of an earlier synthesis. Am. J. Sci. 275-A, 363–396.
Burchfiel, B.C., Fleck, R.J., Secor, D.T., Vincelette, R.R., Davis, G.A., 1974. Geology of the Spring Mountains, Nevada. Geol. Soc. Am. Bull. 85, 1013–1022.
Burchfiel, B.C., Cowan, D.S., Davis, G.A., 1992. Tectonic overview of the Cordilleran orogeny in the western United States. In: Burchfiel, B.C., Lipman, P.W., Zoback, M.L. (Eds.), The Cordilleran Orogen: Conterminous U.S, G-3. Geological Society of America, The Geology of North America, Boulder, Colorado, pp. 407–480.
Cashman, P.H., Trexler Jr., J.H., 1991. The Mississippian Antler Foreland and continental margin in southern Nevada: The Eleana Formation reinterpreted. In: Cooper, J.D., Stevens, C.H. (Eds.), Paleozoic Paleogeography of the western United States-II: Pacific Section SEPM, 67, pp. 271–280.
Cashman, P.H., Villa, D.E., Taylor, W.J., Davydov, V.I., Trexler Jr., J.H., 2011. Late Paleozoic contractional and extensional deformation at Edna Mountain, Nevada. Geol. Soc. Am. Bull. 123, 651–668.
Cashman, P.H., Trexler, J.H., Sturmer, D.M., 2016. Spatial and temporal distribution of Late Paleozoic structures in Nevada: progressive tectonic evolution of the western Laurentian margin. Geol. Soc. Am. Abstr. Programs 48 (7). https://doi.org/10.1130/abs/2016AM-283795.
Cashman, P.H., Grove, S.E., Reid, A.J., Taylor, W.J., 2020. Distinctive west vergence in the Late Paleozoic of north-central Nevada: kinematics and timing. Geol. Soc. Am. Abstr. Programs 52 (4). https://doi.org/10.1130/abs/2020CD-347523.
Castor, S.B., Faulds, J.E., Rowland, S.M., de Polo, C.M., 2000. Geologic map of the Frenchman Mountain Quadrangle, 127. Nevada Bureau of Mines and Geology Map, Clark County, Nevada (Scale 1:24,000).
Chen, N.M., Clemens-Knott, D., 2021. Detrital zircon uranium-lead geochronology of the Schoonover Sequence (Golconda Allochthon, Nevada): alternative paleogeography of the Havallah-Schoonover Basin with implications for Antler-SLaB-Sonoma orogenesis. Palaeogeogr. Palaeoclimatol. Palaeoecol. 575, 110471, 12 p. https://doi.org/10.1016/j.palaeo.2021.110471.
Clapham, M.E., Bishop, J.W., 2010. Arrow canyon and battleship wash field trip: Description of field trip stops. In: Caputo, M.V. (Ed.), The Late Paleozoic Section at Arrow Canyon, Nevada: Facies, Cyclicity, and the Far-Field Record of the Late Paleozoic Ice Age: Upland, California, Pacific Section SEPM (Society for Sedimentary Geology) Book, vol. 109, pp. 8–42.
Cocks, L.R.M., Torsvik, T.H., 2011. The Palaeozoic geography of Laurentia and western Laurussia: a stable craton with mobile margins. Earth Sci. Rev. 106, 1–51. https://doi.org/10.1016/j.earscirev.2011.01.007.
Cole, J.C., Cashman, P.H., 1999. Structural relationships of pre-Tertiary rocks in the Nevada Test Site region, southern Nevada. In: U.S. Geological Survey Professional Paper, 1607, 39 p.
Colpron, M., Nelson, J., 2009. A Palaeozoic Northwest Passage: Incursion of Caledonian, Baltican and Siberian terranes into eastern Panthalassa, and the early evolution of the North American Cordillera. In: Cawood, P.A., Kroner, A. (Eds.), Earth Accretionary Systems in Space and Time: Geological Society of London Special Publication, 318, pp. 273–307.
Crosbie, R.A., 1997. Sequence architecture of Mississippian strata in the White Pine Mountains, White Pine County, Nevada [M.S. Thesis]. University of Nevada, Reno, 257 p.
Currie, B.S., 2002. Structural configuration of the Early Cretaceous cordilleran foreland-basin system and Sevier Thrust Belt, Utah and Colorado. J. Geol. 110, 697–718. https://doi.org/10.1086/342626.
DeCelles, P.G., 2004. Late Jurassic to Eocene evolution of the Cordilleran thrust belt and foreland basin system, western U.S.A. Am. J. Sci. 304, 105–168.
DeCelles, P.G., Coogan, J.C., 2006. Regional structure and kinematic history of the Sevier fold-and-thrust belt, Central Utah. GSA Bull. 118, 841–864. https://doi.org/10.1130/B25759.1.
Dickinson, W.R., 2000. Geodynamic interpretation of Paleozoic tectonic trends oriented oblique to the Mesozoic Klamath-Sierran continental margin in California. In: Soreghan, M.J., Gehrels, G.E. (Eds.), Paleozoic and Triassic Paleogeography and Tectonics of Western Nevada and Northern California: Geological Society of America Special Paper, 347, pp. 209–245.
Dickinson, W.R., Harbaugh, D.W., Saller, A.H., Heller, P.L., Snyder, W.S., 1983. Detrital modes of Upper Paleozoic sandstones derived from Antler Orogen in Nevada: implications for nature of Antler Orogeny. Am. J. Sci. 283, 481–509. https://doi.org/10.2475/ajs.283.6.481.
Domeier, M., Torsvik, T.H., 2014. Plate tectonics in the Late Paleozoic. Geosci. Front. 5, 303–350.
Dott Jr., R.H., 1955. Pennsylvanian stratigraphy of Elko and northern Diamond Ranges, northeastern Nevada. Bull. Am. Assoc. Pet. Geol. 39, 2211–2305.
Dott Jr., R.H., 1958. Cyclic patterns in mechanically deposited Pennsylvanian limestones of northeastern Nevada. J. Sediment. Petrol. 28, 3–14.
Dunne, G.C., Walker, J.D., 2004. Structure and evolution of the Eastern Sierra thrust system, east central California. Tectonics 23, TC4012. https://doi.org/10.1027/2002TC001478.
Erickson, R.L., Marsh, S.P., 1974a. Geologic map of the Iron Point Quadrangle, Humboldt County, Nevada. In: U.S. Geological Survey Geologic Quadrangle Map GQ-1175, 1:24,000.
Erickson, R.L., Marsh, S.P., 1974b. Paleozoic tectonics in the Edna Mountain Quadrangle, Nevada: U.S. Geol. Surv. J. Res. 2 (3), 331–337.
Erickson, R.L., Marsh, S.P., 1974c. Geologic map of the Golconda Quadrangle, Humboldt County, Nevada. In: U.S. Geological Survey Geologic Quadrangle Map GQ-1174, 1:24,000.
Ferguson, H.G., Roberts, R.J., Muller, S.W., 1951. Geology of the Winnemucca quadrangle, Nevada. In: U.S. Geological Survey Geologic Quadrangle Map GQ-11, Scale 1: 125,000.
Ferguson, H.G., Roberts, R.J., Muller, S.W., 1952. Geology of the Golconda quadrangle, Nevada. In: U.S. Geological Survey Geologic Quadrangle Map GQ-15, scale 1: 125,000.
French, D., Walker, J., 2018. Stop 3.2 – Secret Canyon. In: Sturmer, D.M., Cashman, P.H. (Eds.), 2018, Unraveling Tectonic History through Sedimentation and Structural Geology: A Trip in Memory of Jim Trexler, , 2nd ed.vol. NPS-27. Nevada Petroleum and Geothermal Society, Reno, NV, pp. 71–77.
French, D.E., Trexler Jr., J.H., Cashman, P.H., Walker, J.P., Wylie Jr., A.S., 2020. Mississippian mud rocks of the eastern Great Basin: stratigraphy, tectonic significance, and hydrocarbon potential. AAPG Bull. 104, 387–410. https://doi.org/10.1306/05091918190.
Fritz, W.H., 1968. Geologic map and sections of the southern Cherry Creek and northern Egan Ranges, White Pine County, NV. In: Nevada Bureau of Mines and Geology Map, 35 (Scale 1:62,500).
Frye, M.C., Giles, K.A., 2006. Forebulge sourcing of the Mississippian Antler Foreland Basin system: the Tripon Pass Limestone of northwestern Uta and north-central Nevada. In: Harty, K.M., Tabet, D.E. (Eds.), Geology of Northwest Utah, 34. Utah Geological Association Publication, pp. 1–28.
Gamache, M.T., 1986. Fusulinid biostratigraphy of the Bird Spring Formation in the Spring Mountains near Mountain Springs Pass, Clark County, Nevada [M.S. thesis]. Washington State University, Pullman, 215 p.
Gehrels, G.E., Dickinson, W.R., 1995. Detrital zircon provenance of Cambrian to Triassic miogeoclinal and eugeoclinal strata in Nevada. Am. J. Sci. 295, 18–48. https://doi.org/10.2475/ajs.295.1.18.
Gehrels, G.E., Pecha, M., 2014. Detrital zircon U-Pb geochronology and Hf isotope geochemistry of Paleozoic and Triassic passive margin strata of western North America. Geosphere 10, 49–65.
Gehrels, G.E., Blakey, R., Karlstrom, K.E., Timmons, J.M., Dickinson, B., Pecha, M., 2011. Detrital zircon U-Pb geochronology of Paleozoic strata in the Grand Canyon. Arizona: Lithos. 3, 183–200. https://doi.org/10.1130/L121.1.
Giallorenzo, M.A., Wells, M.L., Yonkee, W.A., Stockli, D.F., Wernicke, B.P., 2018. Timing of exhumation, Wheeler Pass thrust sheet, southern Nevada and California: Late Jurassic to middle Cretaceous evolution of the southern Sevier fold-and-thrust belt. Geol. Soc. Am. Bull. 130 (3/4), 558–579. https://doi.org/10.1130/B31777.1.

Giles, K.A., 1996. Tectonically forced retrogradation of the Lower Mississippian Joana Limestone, Nevada and Utah. In: Longman, M.W., Sonnenfeld, M.D. (Eds.), Paleozoic Systems of the Rocky Mountain Region: Rocky Mountain Section/Society of Economic Paleontologists and Mineralogists, pp. 145–164.
Goebel, K.A., 1991. Interpretation of the Lower Mississippian Joana Limestone and implications for the Antler orogenic system [Ph.D. Dissertation]. University of Arizona, Tucson, 222 p.
Grauch, V.J.S., Rodriguez, B.D., Wooden, J.L., 2003. Geophysical and isotopic constraints on crustal structure related to mineral trends in north-central Nevada and implications for tectonic history. Econ. Geol. 98, 269–286.
Guth, P.L., 1981. Tertiary extension north of the Las Vegas Valley shear zone, Sheep and Desert Ranges, Clark County, Nevada. Geol. Soc. Am. Bull. 92, 763–771. https://doi.org/10.1130/0016-7606(1981)92<763:TENOTL>2.0.CO;2.
Harbaugh, D.W., 1980. Depositional facies and provenance of the Mississippian Chainman Shale and Diamond Peak Formation, central Diamond Mountains, Nevada [M.S. thesis]. Stanford University, Stanford, CA, 81 p.
Henderson, C.M., Shen, S.Z., Gradstein, F.M., Agterberg, F.P., 2020. The Permian Period. In: Gradstein, F.M., Ogg, J.G., Schmitz, M., Ogg, G.M. (Eds.), Geologic Time Scale 2020. Elsevier, Amsterdam, pp. 875–902.
Hewett, D.F., 1931. Geology and ore deposits of the Goodsprings quadrangle, Nevada. In: United States Geological Survey Professional Paper, 162, 172 p.
Hose, R.K., Blake, M.C., Jr., and Smith, R.M., 1976, Geology and mineral deposits of White Pine County, Nevada: Nevada Bur. Mine Geol. Bull. 85, 105 p.
Hotz, P.E., Willden, P., 1964. Geology and mineral deposits of the Osgood Mountains quadrangle Humboldt County, Nevada. In: U.S. Geological Survey Professional Paper, 431, 127 p. (scale 1:62,500).
Ingersoll, R.V., Busby, C., Azor Pérez, A., 2012. Tectonics of sedimentary basins, with revised nomenclature. In: Tectonics of Sedimentary Basins: Recent Advances. Wiley-Blackwell, pp. 3–43.
Iverson, B.G., 1991. Stratigraphy of Devonian-Mississippian Rocks, Northern Piñon Range, Southwestern Elko County, Nevada [M.S. Thesis]. University of Nevada, Reno, 88 p.
Jayko, A.S., 2007. Geologic map of the Pahranagat Range 30'x60' Quadrangle. In: Lincoln and Nye Counties, Nevada: USGS SIM-2904 (Scale 1:100,000).
Jones Crafford, A.E., 2008. Paleozoic tectonic domains of Nevada: an interpretive discussion to accompany the geologic map of Nevada. Geosphere 4, 260–291.
Ketner, K.B., 1970. Limestone turbidite of Kinderhook age and its tectonic significance, Elko county, Nevada. In: United States Geological Society Professional Paper 700-D, pp. D18–D22.
Ketner, K.B., 1977. Late Paleozoic orogeny and sedimentation, southern California, Nevada, Idaho and Montana. In: Stewart, J.H., Stevens, C.H., Fritsche, A.E. (Eds.), Paleozoic Paleogeography of the Western United States: Society of Economic Paleontologists and Mineralogists (Society for Sedimentary Geology), Pacific Coast Paleogeography Symposium, 1, pp. 363–369.
Ketner, K.B., Smith, J.F., 1982. Mid-Paleozoic age of the Roberts Mountains thrust unsettled by new data from northern Nevada. Geology 10, 298–303.
Key, E.L., 2015. Paleozoic Structure and Stratigraphy at Iron Point, Humboldt County, North-Central Nevada [M.S. Thesis]. University of Nevada, Reno, 101 p.
Key, E., Cashman, P.H., 2021. Insights from the Golconda Summit area, Nevada: Late Paleozoic structures, regional strike-slip offset, and correlation of the "Comus Formation". In: Henderson, C.M., Snyder, W.S., Ritter, S.M. (Eds.), Tectonostratigraphic Evolution of Pangea's Western Margin: Recent Advances and Remaining Questions, Special Publication, 113. SEPM (Society for Sedimentary Geology), Broken Arrow, Oklahoma. https://doi.org/10.2110/sepmsp.113.08.
Kleinhampl, F.J., Ziony, J.I., 1985. Geology of northern Nye County, Nevada. Nevada Bur. Mine Geol. Bull. 99A, 172 p.
Lane, N.G., 1964. New Pennsylvanian crinoids from Clark County, Nevada. J. Paleontol. 38, 677–684.
Lane, H.R., Brenckle, P.L., Basemann, J.F., Richards, B.C., 1999. The IUGS boundary in the middle of the Carboniferous: Arrow Canyon, Nevada, USA. Episodes 22, 272–283.
Langenheim Jr., R.L., Carss, B.W., Kennerly, J.B., McCutcheon, V.A., Waines, R.H., 1962. Paleozoic section in Arrow Canyon Range, Clark County, Nevada. AAPG Bull. 46, 592–609.
Lawton, T.F., Cashman, P.H., Trexler Jr., J.H., Taylor, W.J., 2017. The late Paleozoic southwestern Laurentian borderland. Geology 45, 675–678. https://doi.org/10.1130/G39071.1.
Leary, R.J., Umhoefer, P., Smith, M.E., Riggs, N., 2017. A three-sided orogen: a new tectonic model for Ancestral Rocky Mountain uplift and basin development. Geology 45, 735–738. https://doi.org/10.1130/G39041.1.
Levy, M., Christie-Blick, N., 1989. Pre-Mesozoic Palinspastic Reconstruction of the Eastern Great Basin (Western United States), 245, pp. 1454–1462. https://doi.org/10.1126/science.245.4925.1454.
Levy, D.A., Zuza, A.V., Haproff, P.J., Odlum, M.L., 2021. Early Permian tectonic evolution of the Last Chance thrust system: an example of induced subduction initiation along a plate boundary transform. GSA Bull. 133, 1105–1127. https://doi.org/10.1130/B35752.1.
Linde, G.M., Cashman, P.H., Trexler Jr., J.H., Dickinson, W.R., 2014. Stratigraphic trends in detrital zircon geochronology of Upper Neoproterozoic and Cambrian strata, Osgood Mountains, Nevada and elsewhere in the Cordilleran miogeocline: Evidence for Early Cambrian uplift of the Transcontinental Arch. Geosphere 10, 1–9.
Linde, G.M., Trexler Jr., J.H., Cashman, P.H., Gehrels, G., Dickinson, W.R., 2016. Detrital zircon U-Pb geochronology and Hf isotope geochemistry of the Roberts Mountains allochthon: new insights into the Early Paleozoic tectonics of western North America. Geosphere 12, 1–16.
Linde, G.M., Trexler Jr., J.H., Cashman, P.H., Gehrels, G., Dickinson, W.R., 2017. Three-dimensional evolution of the early Paleozoic western Laurentian margin: new insights from detrital zircon U-Pb geochronology and Hf-isotope geochemistry of the Harmony Formation of Nevada. Tectonics 36, 2347–2369.
Link, P.K., Warren, I., Preacher, J.M., Skipp, B., 1996. Stratigraphic analysis and interpretation of the Copper Basin Group, McGowan Creek Formation and White Knob Limestone, south-central Idaho. In: Longman, M.W., Sonnenfeld, M.D. (Eds.), Paleozoic Systems of the Rocky Mountain Region: Rocky Mountain Section. SEPM (Society for Sedimentary Geology), pp. 117–144.
Long, S.P., 2012. Magnitudes and spatial patterns of erosional exhumation in the Sevier hinterland, eastern Nevada and western Utah, USA: insights from a Paleogene paleogeographic map. Geosphere 8, 881–901. https://doi.org/10.1130/GES00783.1.
Long, S.P., 2015, An upper-crustal fold province in the hinterland of the Sevier orogenic belt, eastern Nevada, U.S.A.: a Cordilleran Valley and Ridge in the Basin and Range: Geosphere, c. 11, p. 404–424, doi: https://doi.org/10.1130/GES01102.1.
Martin, J.J., 1985. The Webb Formation in the Roberts Mountains, Central Nevada [M.S. Thesis]. University of California, Riverside, 75 p.
Martin, L.G., Montañez, I.P., Bishop, J.W., 2012. A paleotropical carbonate-dominated archive of Carboniferous icehouse dynamics, Bird Spring Fm., southern Great Basin, USA. Palaeogeogr. Palaeoclimatol. Palaeoecol. 329-330, 64–82.
McFarlane, M.J., 1997. The Roberts Mountains thrust in the northern Snake Mountains, Elko County, Nevada. In: Perry, A.J., Abbott, E.W. (Eds.), The Roberts Mountains thrust, Elko and Eureka Counties, Nevada: Nevada Petroleum Society 1997 Field Trip Guidebook, pp. 17–34.
McFarlane, M.J., 2001. Late Paleozoic tectonism in the northern Snake Mountains, Elko County, Nevada [Ph.D. dissertation]. University of Nevada, Reno, 297 p.
McHugh, J.C., 2006. Late Paleozoic contraction in the northern Hot Creek Range, Nye County, Nevada [M.S. Thesis]. University of Nevada, Reno, 107 p.
McKee, E.D., 1982. The Supai Group of Grand Canyon. In: USGS Professional Paper, 1173, 504 p.
McLean, H., 1995. Reconnaissance study of Mississippian siliciclastic sandstones in eastern Nevada. USGS Bull. 1988-I, I1–I19.
McQuarrie, N., Wernicke, B.P., 2005. An animated tectonic reconstruction of southwestern North America since 36 Ma. Geosphere 1, 147–172. https://doi.org/10.1130/GES00016.1.
Miller, R.P., Heller, P.L., 1994. Depositional framework and controls on mixed carbonate-siliciclastic gravity flows: Pennsylvanian-Permian shelf to basin transect, southwestern Great Basin, USA. Sedimentology 41, 1–20.
Mollazal, Y., 1961. Petrology and petrography of Ely Limestone in part of eastern Great Basin. In: Provo, Utah, Brigham Young University Geology Studies, 8, pp. 3–35.
Nelson, J.L., Colpron, M., Piercey, S.J., Dusel-Bacon, C., Murphy, D.C., Roots, C.F., 2006. Paleozoic tectonic and metallogenic evolution of the pericratonic terranes in Yukon, northern British Columbia and eastern Alaska. In: Colpron, M., Nelson, J.L. (Eds.), Paleozoic Evolution and Metallogeny of Pericratonic Terranes at the Ancient Pacific Margin of North America, Canadian and Alaskan Cordillera: Geological Association of Canada, Special Paper, vol. 45, pp. 323–360.
Nilsen, T.H., Stewart, J.H., 1980. The Antler Orogeny – Mid-Paleozoic tectonism in western North America. Geology 8, 298–302.
Nutt, C.J., Hart, K.S., 2004. Geologic map of the Big Bald Mountain Quadrangle and part of the Tognini Spring Quadrangle, White Pine County, Nevada. In: Nevada Bureau of Mines and Geology Map, 145 (Scale 1:24,000).
Otto, B.R., 2008. Geologic map of the Central Butte Range, White Pine County, Nevada. In: Nevada Bureau of Mines and Geology Map, 160 (Scale 1:48,000).
Oversby, B., 1973. New Mississippian formation in northeastern Nevada and its possible significance. Am. Assoc. Petrol. Geol. 57 (9), 1779–1783.
Page, W.R., Lundstrom, S.C., Harris, A.G., Langenheim, V.E., Workman, J.B., Mahan, S. A., Paces, J.B., Dixon, G.L., Rowley, P.D., Burchfiel, B.C., Bell, J.W., Smith, E.I., 2005. Geologic and geophysical maps of the Las Vegas 30'x60' quadrangle, Clark and Nye Counties, Nevada, and Inyo County, California. In: United States Geological Survey Scientific Investigations Map, 2814 (scale 1:100,000).
Payne, J.D., Schiappa, T., 2000. Biostratigraphic characterization and tectonostratigraphic implications of a newly recognized middle Pennsylvanian unit, Buck Mountain, White Pine County, Nevada. Geological Society of America Abstracts with Programs 35 (5), 36.
Pérez-Huerta, A., 2004. Brachiopods and Paleoecological Studies in the Pennsylvanian of the Great Basin (U.S.A.) [Ph.D. dissertation]. University of Oregon, Eugene, 419 p.
Perry, A.J., 1994. Stratigraphic and Sedimentologic Analysis of the (Upper Mississippian) lower Newark Valley Sequence, Diamond Range, Eureka and White Pine Counties, Nevada [M.S. Thesis]. University of Nevada, Reno, 243 p.
Pfefferkorn, H.W., 1972. Distribution of *Stigmaria wedingtonensis* (Lycopsida) in the Chesterian (Upper Mississippian) of North America. Am. Midl. Nat. 88, 225–231.
Phillips, T.L., DiMichele, W.A., 1992. Comparative ecology and life-history biology of arborescent lycopsids in Late Carboniferous swamps of Euramerica. Ann. Missouri Botanical Gardens 79, 560–588.
Poole, F.G., 1974. Flysch deposits of the Antler foreland basin, western United States. In: Dickinson, W.R. (Ed.), Tectonics and Sedimentation: Society of Economic Paleontologists and Mineralogists Special Publication, 22, pp. 58–82.
Rice, J.A., 1990. Stratigraphy, Diagenesis, and Provenance of Upper Paleozoic Eolian Limestones, Western Grand Canyon and Southern Nevada [Ph.D. dissertation]. University of Nebraska, Lincoln, NE, 147 p.
Ritter, S.M., Robinson, T.S., 2009. Sequence stratigraphy and biostratigraphy of Carboniferous-Permian boundary strata in western Utah. In: Tripp, B.T., et al. (Eds.), Geology and Geologic Resources and Issues of Western Utah, 38. Utah Geological Association, Salt Lake City, UT, pp. 27–42.

Roberts, R.J., 1964. Stratigraphy and structure of the Antler Peak Quadrangle Humboldt and Lander Counties Nevada. In: USGS Professional Paper 459-A, pp. A1–A93.
Roberts, R.J., 1968. Tectonic framework of the Great Basin: University of Missouri. Rolla J. 1 (1), 101–119.
Roberts, R.J., Hotz, P.E., Gilluly, J., Ferguson, H.G., 1958. Paleozoic rocks of north-central Nevada. Am. Assoc. Pet. Geol. Bull. 42 (12), 2813–2857.
Robinson Jr., G.B., 1961. Stratigraphy and Leonardian fusulinid paleontology in central Pequop Mountains, Elko County, Nevada, 8. Brigham Young University Geology Studies, pp. 93–145.
Ross, C.A., Ross, J.P.R., 1987. Late Paleozoic sea levels and depositional sequences. In: Ross, C.A., Haman, D. (Eds.), Timing and Depositional History of Eustatic Sequences: Constraints on Seismic Stratigraphy: Cushman Foundation for Foraminiferal Research special publication, 24, pp. 137–150.
Russo, A.G., 2013. Pennsylvanian to Cretaceous Folds and Thrusts in South-central Nevada: Evidence from the Timpahute Range [M.S. Thesis]. University of Nevada, Las Vegas, 87 p.
Russo, A.G., Taylor, W.J., Cashman, P.H., 2021. Late Paleozoic shortening in south-Central Nevada using regional correlations of major pre-Sevier structures. In: Henderson, C.M., Snyder, W.S., Ritter, S.M. (Eds.), Tectonostratigraphic Evolution of Pangea's Western Margin: Recent Advances and Remaining Questions, Special Publication, 113. SEPM (Society for Sedimentary Geology), Broken Arrow, Oklahoma. https://doi.org/10.2110/sepmsp.113.05.
Saller, A.H., Dickinson, W.R., 1982. Alluvial to marine facies transition in the Antler Overlap sequence, Pennsylvanian and Permian of north-central Nevada. J. Sediment. Petrol. 52, 925–940.
Saltzman, M.R., 2003. Late Paleozoic ice age: oceanic gateway or $pCO_2$? Geology 31, 151–154.
Sandberg, C.A., Morrow, J.R., Ziegler, W., 2002. Late Devonian Sea-level changes, catastrophic events, and mass extinctions. In: Koeberl, C., MacLeod, K.G. (Eds.), Catastrophic Events and Mass Extinctions: Impacts and Beyond, 356. Geological Society of America Special Paper, Boulder, Colorado, pp. 473–487.
Early Mississippian sequences at Union Pass, Elko and Eureka counties, Nevada. In: Saucier, A.E., Hansen, M.W., Walker, J.P., Trexler Jr., J.H. (Eds.), 1995. 1995, Mississippian Source Rocks in the Antler Basin of Nevada and Associated Stratigraphic and Structural Traps: 1995 Fieldtrip Guidebook. Nevada Petroleum Society, Inc, Reno, Nevada, 165 p.
Saucier, A.E., 1997. The Antler thrust system in northern Nevada. In: Perry, A.J., Abbott, E.W. (Eds.), The Roberts Mountains Thrust, Elko and Eureka Counties. Nevada Petroleum Society 1997 Field Trip Guidebook, Nevada, pp. 1–16.
Schattauer, S.A., Schiappa, T.A., 2010. New Pennsylvanian Somoholitid species from White Pine County, Nevada. Geol. Soc. Am. Abstr. Programs 42 (1), 125.
Schiappa, T.A., Spinosa, C., Snyder, W., Davydov, V., 2017. Using Late Paleozoic ammonoids as proxies for basin development and characterization along the western margin of the United States. Geol. Soc. Am. Abstr. Programs 49 (6). https://doi.org/10.1130/abs/2017AM-305505.
Scott, L.A., Elrick, M.B., 2004. Cycle and sequence stratigraphy of middle Pennsylvanian (Desmoinesian) strata of the Lucero basin, Central New Mexico. In: Lucas, S.G., Zeigler, K.E. (Eds.), Carboniferous –Permian Transition. New Mexico Museum of Natural History and Science Bulletin No. 25, Albuquerque, pp. 31–42.
Siebenaler, S.A., 2011. Late Paleozoic Deformation in the Osgood Mountains and Dry Hills, northern Nevada [M.S. thesis]. University of Nevada, Las Vegas, 176 p.
Silberling, N.J., Roberts, R.J., 1962. Pre-Tertiary stratigraphy and structure of northwestern Nevada. In: Geological Society of America Special Paper, 72, 58 p.
Silberling, N.J., Nichols, K.M., Trexler Jr., J.H., Jewell, P.W., Crosbie, R.A., 1997. Overview of Mississippian depositional and paleotectonic history of the Antler foreland, eastern Nevada and western Utah. In: Link, P.K., Kowalis, B.J. (Eds.), Geological Society of America Fieldtrip Guidebook. Brigham Young University, Provo, pp. 161–196.
Smith, J.F., Ketner, K.B., 1968. Devonian and Mississippian rocks and the date of the Roberts Mountains thrust in the Carlin-Pinon Range area, Nevada. USGS Bull. 1251-I, 11–118.
Snow, J.K., 1992. Large magnitude Permian shortening and continental-marginal tectonics in the southern Cordillera. Geol. Soc. Am. Bull. 104, 80–105.
Snow, J.K., Wernicke, B.P., 2000. Cenozoic tectonism in the central Basin and Range: magnitude, rate, and distribution of upper crustal strain. Am. J. Sci. 300, 659–719.
Snyder, W.S., Brueckner, H.K., 1983. Tectonic evolution of the Golconda Allochthon, Nevada: Problems and perspectives. In: Stevens, C.H. (Ed.), Pre-Jurassic Rocks in Western North American Suspect Terranes: Upland, California, Pacific Section-SEPM book, 32, pp. 103–123.
Snyder, W.S., Trexler Jr., J.H., Cashman, P.H., Davydov, V.I., 2000. Tectonostratigraphic Framework of the Upper Paleozoic Continental Margin of Nevada and Southeastern California: Reno, Geological Society of Nevada Program with Abstracts, pp. 76–77.
Snyder, W.S., Trexler Jr., J.H., Davydov, V.I., Cashman, P., Schiappa, T.A., Sweet, D., 2002. Upper Paleozoic tectonostratigraphic framework for the western margin of North America. In: AAPG Hedberg Conference, Proceedings, Late Paleozoic Tectonics and Hydrocarbon Systems of Western North America - The Greater Ancestral Rocky Mountains. American Association of Petroleum Geologists, Tulsa, 4 p. (unpaginated). http://www.searchanddiscovery.net/abstracts/pdf/2003/2002hedberg_vail/ndx_snyder.pdf.
Speed, R.C., Sleep, N.H., 1982. Antler orogeny and foreland basin: a model. Geol. Soc. Am. Bull. 93, 815–828. https://doi.org/10.1130/0016-7606(1982)93<815:AOAFBA>2.0.CO;2.
St. Aubin-Hietpas, L.A., 1983. Carbonate Petrology and Paleoecology of Permo-Carboniferous Rocks, southwestern Millard County, Utah, 30. Brigham Young University Geology Studies, Provo, Utah, pp. 113–143.
Stevens, C.H., Stone, P., 2007. The Pennsylvanian-Early Permian Bird Spring carbonate shelf, southeastern California: fusulinid biostratigraphy, paleogeographic evolution, and tectonic implications. Geol. Soc. Am. Spec. Pap. 429, 82 p.
Stevens, C.H., Stone, P., Belasky, P., 1991. Paleogeographic and structural significance of an Upper Mississippian facies boundary in southern Nevada and east-central California. Geol. Soc. Am. Bull. 103, 876–885.
Stevens, C.H., Klingman, D.S., Sandberg, C.A., Stone, P., Belasky, P., Poole, F.G., Snow, J. K., 1996. Mississippian stratigraphic framework of east-central California and southern Nevada with revision of Upper Devonian and Mississippian stratigraphic units in Inyo County, California. U.S. Geol. Surv. Bull. 1988-J, 39 p.
Stevens, C.H., Stone, P., Ritter, S.M., 2001. Conodont and Fusulinid Biostratigraphy and History of the Pennsylvanian to Lower Permian Keeler Basin, East-central California, 46. Brigham Young University Geology Studies, Provo, Utah, pp. 99–142.
Stevens, C.H., Stone, P., Magginetti, R.T., Ritter, S.M., 2015. Stratigraphy and paleogeographic significance of a Late Pennsylvanian to Early Permian channeled slope sequence in the Darwin Basin, southern Darwin Hills, east-central California. Stratigraphy 12 (2), 185–196.
Stone, P., Stevens, C.H., 1988. Pennsylvanian and Early Permian paleogeography of east-central California: implications for the shape of the continental margin and the timing of continental truncation. Geology 16, 330–333.
Sturmer, D.M., 2012. Stable Carbon Isotope Chemostratigraphy and Tectonic Setting of the Pennsylvanian Ely-Bird Spring Basin, Nevada and Utah: Interpreting Three-Dimensional Basin Evolution using Multiple Stratigraphic Techniques [Ph.D. dissertation]. University of Nevada, Reno, Reno, 378 p.
Sturmer, D.M., Trexler Jr., J.H., Poulson, S.R., 2012. Carbonate-carbon isotope stratigraphy and three-dimensional subsidence history of the Pennsylvanian Ely-Bird Spring basin, Nevada and Utah. Geol. Soc. Am. Abstr. Programs 44 (6), 23.
Sturmer, D.M., Trexler Jr., J.H., Cashman, P.H., 2018. Tectonic analysis of the Pennsylvanian Ely-Bird Spring Basin: Late Paleozoic tectonism on the southwestern Laurentia margin and the distal limit of the Ancestral Rocky Mountains. Tectonics 37, 604–620. https://doi.org/10.1002/2017TC004769.
Sturmer, D.M., Cashman, P.H., Trexler Jr., J.H., Poulson, S.R., 2021. Evolution of the Pennsylvanian Ely-Bird Spring basin: insights from carbon isotope stratigraphy. In: Henderson, C.M., Snyder, W.S., Ritter, S.M. (Eds.), Tectonostratigraphic Evolution of Pangea's Western Margin: Recent Advances and Remaining Questions, Special Publication, 113. SEPM (Society for Sedimentary Geology), Broken Arrow, Oklahoma. https://doi.org/10.2110/sepmsp.113.04.
Sur, S., Soreghan, G.S., Soreghan, M.J., Yang, W., Saller, A.H., 2010. A record of glacial aridity and Milankovitch-scale fluctuations in atmospheric dust from the Pennsylvanian tropics. J. Sediment. Res. 80, 1046–1067. https://doi.org/10.2110/jsr.2010.091.
Sweet, D., 2003. The Late Paleozoic Tectonostratigraphy of the Central Pequop Mountains, Elko County, Nevada [M.S. thesis]. Boise State University, 130 p.
Taylor, W.J., Bartley, J.M., Martin, M.W., Geissman, J.W., Walker, J.D., Armstrong, P.A., Fryxell, J.E., 2000. Relations between hinterland and foreland shortening, Sevier orogeny, central North American Cordillera. Tectonics 19, 1124–1143.
Thorman, C.H., Brooks, W.E., 2011. Bedrock geology of the ranges bounding the Wells Earthquake of February 21, 2008. In: Nevada Bureau of Mines and Geology Special Publication, 36, pp. 65–78.
Tierney, K.E., 2005. Carbon Isotopic Response to Oceanographic Changes at Milankovitch Scale Periodicity in Pennsylvanian Limestones from Arrow Canyon, Nevada [M.S. thesis]. The Ohio State University, Columbus, 46 p.
Titus, A.L., 1992. Mid-Carboniferous Biostratigraphy and Ammonoid Paleontology of the Upper Eleana Formation (Unit J, Upper Quartzite subunit), Syncline Ridge [M.S. thesis]. University of Arkansas, Fayetteville, 135 p.
Titus, A.L., Manger, W.L., 1992. Mid-Carboniferous (E2c-H1b) ammonoid biostratigraphy, Nevada Test Site, Nye County, Nevada. GSA Abstr. Progr. 24 (6), 66.
Trexler Jr., J.H., Cashman, P.H., 1991. Mississippian stratigraphy and tectonics of east-central Nevada. In: Cooper, J.D., Stevens, C.H. (Eds.), Paleozoic Paleogeography of the Western United States—II: Pacific Section SEPM, 67, pp. 331–342.
Trexler Jr., J.H., Cashman, P.H., 1997. A southern Antler foredeep submarine fan: the Mississippian Eleana Formation, Nevada Test Site. J. Sediment. Res. 67 (6), 1044–1059.
Trexler Jr., J.H., Nitchman, S.P., 1990. Sequence stratigraphy and evolution of the Antler foreland basin, east-central Nevada. Geology 18, 422–425.
Trexler Jr., J.H., Snyder, W., Schwarz, D., Teru Kurka, M., Crosbie, R., 1995. An overview of the Mississippian Chainman Shale. In: Hansen, M.W., Walker, J.P., Trexler Jr., J. H. (Eds.), Mississippian Source Rocks in the Antler Basin of Nevada and Associated Structural and Stratigraphic Traps: Nevada Petroleum Society 1995 Field Trip Guidebook, pp. 45–60.
Trexler Jr., J.H., Cole, J.C., Cashman, P.H., 1996. Middle Devonian-Mississippian stratigraphy on and near the Nevada Test Site: implications for hydrocarbon potential. AAPG Bull. 80, 1736–1762.
Trexler Jr., J.H., Cashman, P.H., Cole, J.C., Snyder, W.S., Tosdal, R.M., Davydov, V.I., 2003. Widespread effects of middle Mississippian deformation in the Great Basin of western North America. Geol. Soc. Am. Bull. 115, 1278–1288.
Trexler Jr., J.H., Cashman, P.H., Snyder, W.S., Davydov, V.I., 2004. Late Paleozoic tectonism in Nevada: timing, kinematics, and tectonic significance. Geol. Soc. Am. Bull. 116, 525–538.
Villa, D.E., 2007. Late Paleozoic deformation at Edna Mountain, Humboldt County, Nevada [M.S. Thesis]. University of Nevada, Reno, 122 p.
Walker, J.D., 1988. Permian, and Triassic rocks of the Mojave Desert and their implications for timing and mechanisms of continental truncation. Tectonics 7, 685–709.
Webster, G.D., Lane, N.G., 1967. Mississippian-Pennsylvanian boundary in southern Nevada. In: Teichert, C., Yochelson, E.L. (Eds.), Essays I Paleontology and

Stratigraphy, R.C. Moore Commemorative Volume, 2. University of Kansas Special Publication, pp. 502–522.
Webster, G.D., Lane, N.G., 1970. Carboniferous echinoderms from the southwestern United States. J. Paleontol. 44, 276–296.
Welsh, J.E., 1959. Biostratigraphy of the Pennsylvanian and Permian Systems in Southern Nevada [Ph.D. dissertation]. Salt Lake City, University of Utah, 106 p. + app.
Whitmore, R.J., 2011. Mid- to Late-Paleozoic deformation on Buck Mountain, White Pine County, Nevada [M.S. thesis]. Reno, University of Nevada, Reno, 101 p.
Whitmore, R.J., Cashman, P.H., Sturmer, D.M., 2021. Structures at Buck Mountain, Nevada: Establishing the southeastern extent of mid-Pennsylvanian tectonism. In: Henderson, C.M., Snyder, W.S., Ritter, S.M. (Eds.), Tectonostratigraphic Evolution of Pangea's Western Margin: Recent Advances and Remaining Questions, Special Publication, 113. SEPM (Society for Sedimentary Geology), Broken Arrow, Oklahoma. https://doi.org/10.2110/sepmsp.113.06.
Wilson, E., Preacher, J.M., Link, P.K., 1994. New constraints on the nature of the Early Mississippian Antler sedimentary basin in Idaho. In: Embry, A.F., Beauchamps, B., Glass, D.J. (Eds.), Pangea: Global Environments and Resources, 17. Canadian Society of Petroleum Geologists Memoir, pp. 155–174.
Wise, D., 1977. Paleozoic Geology of the Dobbin Summit-Clear Creek area, Monitor Range, Nye County, Nevada [M.S. thesis]. Oregon State University, Corvallis, 137 p.
Yose, L.A., Heller, P.L., 1989. Sea-level control of mixed-carbonate-siliciclastic, gravity-flow deposition: lower part of the Keeler Canyon Formation (Pennsylvanian), southeastern California. Geol. Soc. Am. Bull. 101, 427–439.